Bundeswehr Hospital Ulm
Institute of Pathology and Molecular Pathology
Director: Prof. Dr. med. Dr. rer. nat. Konrad Steinestel

Clinical, Histopathological, and Radiological Characterization of Post-Acute Sequelae of COVID-19

Dissertation to obtain the

Doctoral Degree in Dentistry (Dr. med. dent.) at the Medical Faculty of Ulm

University

submitted by

Annika Czech

Ulm

2024

Incumbent Dean: Prof. Dr. rer. nat. Thomas Wirth
1. First Reporter: Prof. Dr. med. Dr. rer. nat. Konrad Steinestel
2. Second Reporter: Prof. Dr. med. Dominik Buckert
Date of Defense: 16.01.2025

Results gained in this dissertation have previously been published in the following:

Gagiannis D, Czech A, Steinestel K (2022) Post-COVID: The multimodal path to the right treatment strategy. ERJ Open Research 8: 80. doi: 10.1183/23120541.LSC-2022.80

Gagiannis D, Hackenbroch C, Czech A, Lindner A, Maag N, Bloch W, Zech F, Kirchhoff F, Djudjaj S, Stillfried S von, Bülow R, Boor P, Steinestel K: Clinical, imaging, serological, and histopathological features of pulmonary post-acute sequelae after mild COVID-19 (PASC). MedRxiv (Preprint). https://www.medrxiv.org/content/10.1101/2022.11.29.22282913v1 (08.03.2023)

Steinestel K, Czech A, Hackenbroch C, Bloch W, Gagiannis D (2021) Klinische, radiologische und histopathologische Merkmale des pulmonalen Post-COVID-Syndroms. Pathologe 42:160–164. doi: 10.1007/s00292-021-01024-6

Table of Contents

Abbreviations III

1.0.0 Introduction ***1***

1.1.0 Virology 2

1.2.0 Structure 3

1.3.0 Pathogenesis 5

1.4.0 Transmission and Epidemiology 5

1.5.0 Acute COVID-19 7

1.6.0 Post-acute Sequelae of COVID-19 (PASC) 11

1.7.0 Possible Causes of PASC 15

1.8.0 Post-viral Pulmonary Diseases 16

1.9.0 Interstitial Pneumonia with Autoimmune Features (IPAF) 21

2.0.0 Material and Methods ***24***

2.1.0 Patients and Diagnostics Workup 24

2.2.0 Serology 24

2.3.0 Histology and Sars-CoV-2 Detection 25

2.4.0 Spiroergometry 25

2.5.0 Radiology 30

2.6.0 Bronchoscopy and Lung Sampling 30

3.0.0 Results ***34***

3.1.0 General Cohort Characteristics 34

3.2.0 Diagnostic Scheme 34

3.3.0 Clinical Results 36

3.4.0 Imaging Results 38

3.5.0 Serological results 39

3.6.0 Histopathological Findings and Tissue-based SARS-CoV-2 Detection 39

3.7.0 Spatial T-lymphocyte Subtyping in PASC Patients and Autopsy Controls. 43

3.8.0 Assessment of Interstitial Fibrosis and Quantification of Macrophage Subpopulations in PASC Patients. 45

4.0.0 Discussion ***49***

4.1.0 Data Analysis: The Link of PASC to Elevated Autoantibodies and T-cells 50

4.2.0 The Link Between Persisting Viral Components and Chronic Inflammation 50

4.3.0 Do Antibodies and Cytokines Play a Role in the Development of PASC, and If Yes, How? 51

4.4.0 What is the Cause of Pulmonary PASC? 52

4.5.0 Limitations 53

5.0.0 Summary 55

6.0.0 Bibliography 57

Appendix 63

Acknowledgment 66

Curriculum Vitae 67

Abbreviations

ACE2 - Angiotensin-Converting Enzyme 2

ANA - Antinuclear Antibodies

ANAs/ENAs - Anti-Nuclear/Anti-Extractable Nuclear Antibodies

ANCA - Anti-Neutrophil Cytoplasmic Antibodies

Anti-CCP - Anti-Cyclic Citrullinated Peptide

Anti-dsDNA - Anti-Double-Stranded DNA

Anti-MPO - Anti-Myeloperoxidase

Anti-PM-Scl - Anti-Polymyositis/Scleroderma

Anti-PR3 - Anti-Proteinase 3

Anti-RNP - Anti-Ribonucleoprotein

Anti-Scl-70 - Anti-Topoisomerase

ARDS - Acute Respiratory Distress Syndrome

BAL - Bronchoalveolar Lavage

bpm - Beats Per Minute

CD - Cluster of Differentiation

c-ANCA - Cytoplasmic Anti-Neutrophil Cytoplasmic Antibodies

COPD - Chronic Obstructive Pulmonary Disease

CoV - Coronavirus

COVID-19 - Coronavirus Disease 2019

CT - Computed Tomography

CTD - Connective Tissue Diseases

CTD-ILD - Connective Tissue Disease-Associated Interstitial Lung Disease

DAD - Diffuse Alveolar Damage

DC - Dendritic Cell

DECT - Dual-Energy Computed Tomography

DLCO - Diffusing Capacity of the Lung for Carbon Monoxide

dsDNA - Double-Stranded DNA

E - Envelope protein

ECG - Electrocardiogram

ENA - Extractable Nuclear Antigen

EvG - Elastica-van-Gieson

FEV1 - Forced Expiratory Volume in One Second

FFPE - Formalin-Fixed Paraffin-Embedded

FISH - Fluorescence In Situ Hybridization

FVC - Forced Vital Capacity

GGO - Ground-Glass Opacities

GIT - Gastrointestinal Tract

HAV - High Attenuation Volume

hACE2 - Human Angiotensin-Converting Enzyme 2

HE - Hematoxylin and Eosin

HF - Heart Frequency

HCoV-229E - Human Coronavirus 229E

HCoV-HKU1 - Human Coronavirus HKU1

HCoV-NL63 - Human Coronavirus NL63

HCoV-OC43 - Human Coronavirus OC43

HRCT - High-Resolution Computed Tomography

HU - Hounsfield Units

IFN - Interferon

IFN-λ1 - Interferon Lambda 1

IgE - Immunoglobulin E

IL - Interleukin

IL-6 - Interleukin 6

ILD - Interstitial Lung Disease

IIF - Indirect Immunofluorescence

IPAF - Interstitial Pneumonia with Autoimmune Features

IQR - Interquartile Range

LABA - Long-Acting Beta2 Agonists

LAV - Low Attenuation Volume

LTRA - Leukotriene Receptor Antagonists

M - Membrane glycoprotein

MEF50 - Maximal Expiratory Flow at 50% of FVC

MERS-CoV - Middle East Respiratory Syndrome Coronavirus

MG - Masson-Goldner

MHC - Major Histocompatibility Complex

mm^2 - Square Millimeters

mmHg - Millimeters of Mercury

MSI - Multispectral Imaging

N - Nucleocapsid protein

NICE - National Institute for Health and Care Excellence

NSIP - Nonspecific Interstitial Pneumonia

ORF - Open Reading Frames

PASC - Post-Acute Sequelae of SARS-CoV-2 Infection

PBS - Phosphate Buffered Saline

PCR - Polymerase Chain Reaction

PetCO2 - End-Tidal Partial Pressure of Carbon Dioxide

PetO2 - End-Tidal Partial Pressure of Oxygen

PCNA - Proliferating Cell Nuclear Antigen

PM-Scl - Polymyositis/Scleroderma

p-ANCA - Perinuclear Anti-Neutrophil Cytoplasmic Antibodies

RBD - Receptor Binding Domain

REACT - WHO Rapid Evidence Appraisal for COVID-19 Therapies

RER – Respiratory

RKI - Robert Koch Institute

RdRp - RNA-Dependent RNA Polymerase

S - Spike protein

S1 - Subunit 1 of the Spike protein

S2 - Subunit 2 of the Spike proteinSABA - Short-Acting Beta2 Agonists

SARS-CoV-1 - Severe Acute Respiratory Syndrome Coronavirus 1

SARS-CoV-2 - Severe Acute Respiratory Syndrome Coronavirus 2

Scl-70 - Topoisomerase antibody

SpO2 - Peripheral Capillary Oxygen Saturation

SS-B - Sjögren's syndrome-related antigen B

ssRNA - Single-Stranded RNA

TBB - Transbronchial Biopsy

TCR - T-cell Receptor

TEM - Transmission Electron Microscopy

Th2 - T helper-2 cells

TLC - Total Lung Capacity

TNF-α - Tumor Necrosis Factor alpha

TMPRRS2 - Transmembrane Serine Protease 2

VC - Vital Capacity

VE/VECO2 - Ventilatory Equivalent for Carbon Dioxide

VE/VEO2 - Ventilatory Equivalent for Oxygen

VO2 - Volume of Oxygen

VO2/HF - Volume of Oxygen per Heartbeat (interpreted)

VO2max - Maximum Oxygen Uptake

VCO2 - Volume of Carbon Dioxide

WHO - World Health Organization

x-ANCA - Atypical Anti-Neutrophil Cytoplasmic Antibodies

1.0.0 Introduction

SARS-CoV-2, or "severe acute respiratory syndrome coronavirus 2," is responsible for the ongoing widespread COVID-19 pandemic, believed to have originated in Wuhan, China, in 2019. COVID-19, which stands for Corona Virus Disease 2019, results from an infection with SARS-CoV-2. Patients commonly exhibit symptoms in the upper respiratory tract, gastrointestinal tract, central nervous system, and liver. (Shanmugam *et al.*, 2020; Gagiannis *et al.*, 2023)

The disease presents a wide range of severity, from milder symptoms resembling the common cold to the more critical acute respiratory distress syndrome (ARDS), which can often be life-threatening. In severe cases progressing to ARDS, reports have noted diffuse alveolar damage (DAD) accompanied by fibromyxoid exudates, desquamation of pneumocytes, hyaline membrane formation, and lung edema. (Xu *et al.*, 2020) Recovery occurs within four weeks. Yet, around 30% of patients exhibit lingering symptoms post-viral clearance. (Proal and VanElzakker, 2021) Acute COVID-19 is characterized by symptoms lasting up to four weeks. The NICE guidelines categorize symptoms persisting between 4 to 12 weeks as ongoing symptomatic COVID-19. Beyond twelve weeks, its ongoing symptoms are termed post-COVID-19 syndrome.

Consequently, the designations "long-covid" or post-acute sequelae of SARS-CoV-2 infection (PASC) aren't explicitly defined by the NICE guidelines. Still, they are popularly utilized to describe symptom patterns from the fourth week onwards (National Institute for Health and Care Excellence (NICE), 2023). PASC encompasses many clinical manifestations, with fatigue and dyspnoea being the most common—field (National Institute for Health and Care Excellence (NICE), 2023). Presently, there is an information gap concerning the precise mechanisms driving PASC. Notably, PASC shares numerous clinical presentations with other virus-induced respiratory illnesses. To pinpoint specific clinical patterns PASC might have in common with recognized diseases and to better understand its exact mechanism, the clinical, histopathological, and radiological characteristics of PASC were concluded.

1.1.0 Virology

SARS CoV-2 belongs to the family of Corona Virus (*Coronaviridae*). They are RNA (+), enveloped, single-stranded viruses. SARS-CoV-2 belongs to the Coronaviridae family. These are RNA (+), enveloped, single-stranded viruses. "Coronaviridae" derives from the Latin word "Corona," which means crown. (Su *et al.*, 2016)

The Coronavirus family can be further categorized into four genera, as depicted in **Figure 1**.
Firstly, Alphacoronavirus and Betacoronavirus primarily affect humans and mammals. Secondly, Gammacoronavirus and Deltacoronavirus are mainly associated with avian species hosts. Typically, the β-genera cause respiratory symptoms in humans, a hallmark of the current SARS-CoV-2 pandemic. (Cui, Li and Shi, 2019)

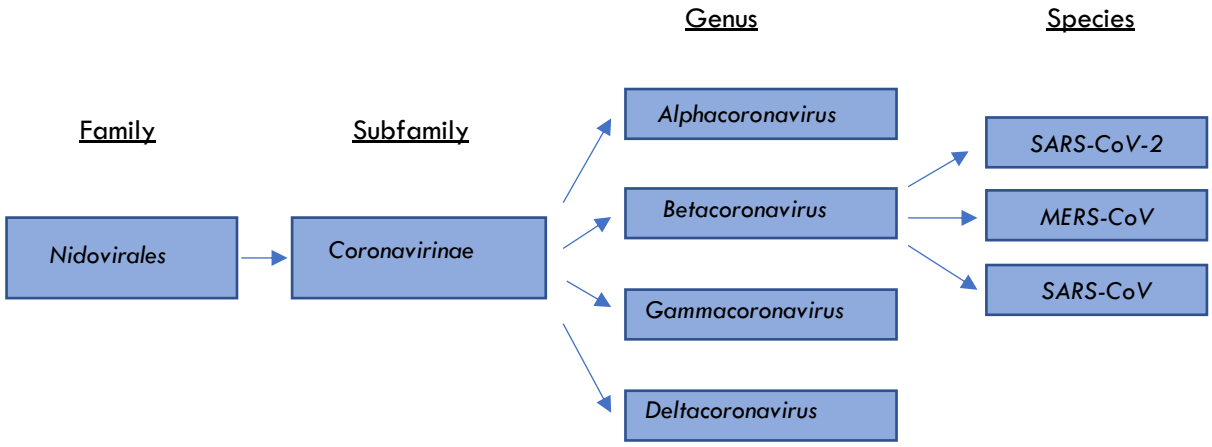

Figure 1 The viral taxonomy of SARS-CoV-2 subcategorized into family, subfamily, genus, and species. *Severe Acute Respiratory Syndrome Coronavirus 2 (SARS-CoV-2), Middle East Respiratory Syndrome Coronavirus (MERS-CoV), Severe Acute Respiratory Syndrome Coronavirus (SARS-CoV)*

Currently, six *Coronaviridae* that are known to infect humans: (HCoV-229E (229E), HCoV-OC43 (OC43), (SARS-CoV), HCoV-NL63 (NL63), HCoV-HKU1 (HKU1), and (MERS-CoV)). (Su *et al.*, 2016)

1.2.0 Structure

The virions have a helical nucleocapsid and are spherical with an enveloped single-stranded RNA (ssRNA). Among RNA viruses, they possess one of the largest genomes, ranging from 26 to 32 kb. These virions measure about 60-140nm in diameter. (Mittal *et al., 2020; Masters, 2006)* They also feature 5' caps and 3' poly(A) tails, resembling most eukaryotic mRNA structures. This similarity is beneficial as the virion's RNA serves as an mRNA to be translated into a substantial replicase protein. However, in contrast to eukaryotic mRNA, the presence of Open Reading Frames (ORF) is notable within the genome. Its primary section adjacent to the 5'-cap codes for 16 different non-structural proteins to aid in viral genome replication. The latter portion of the ORF, closer to the 3' end, encodes structural proteins such as the Envelope (E), Spike (S), Membrane glycoprotein (M), and Nucleocapsid (N) proteins **(Figure 2)** (Shanmugam *et al.*, 2020)(Riefaie, 2020) (Masters, 2006)

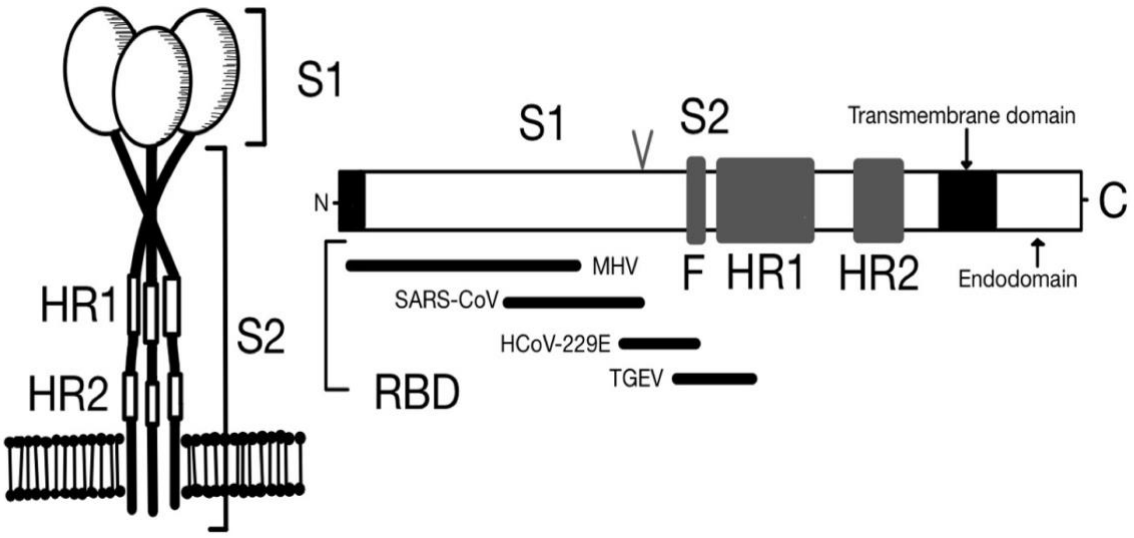

Figure 2 The structure of a spike protein (S). *On the left side the location of the heptad repeat region1 and 2 (HR1) and (HR2) within the S2 (carboxy-terminal) can be seen. The structure of S1 and S2 is depicted on the right. S1 is the amino-terminal and S2 the carboxy-terminal. The arrow signifies where the molecule is split by proteases. Receptor-binding domains (RBDs) are located in S1 as seen on the right. A more detailed outline of the fusion peptide (F), endodomain and transmembrane domain is visible on the right. (Masters, 2006)*

The spike protein (S protein) is located on the virion envelope, giving the virus its unique shape and name, and has a length of 9-12nm (Masters, 2006). It consists of a transmembrane, endo-, and ectodomain, forming trimers, which are also heavily glycosylated. The ectodomain stands out as the spike's most extensive and prominent segment. The entire spike can be divided into S1 and S2. While S1 contains an RBD (Ribosome Binding Domain) and a signaling peptide to bind to the host's ACE2 receptor, S2 manages the fusion of the envelope with the host cell's membrane, encompassing a putative fusion peptide and two heptad repeat regions. (**Figure 2)** (Masters, 2006)(Riefaie, 2020)

The Envelope (E) Protein is an essential membrane protein forming the mentioned envelope. Meanwhile, the Nucleocapsid (N) Protein associates with the viral RNA, structuring it similarly to beads on a string. (Riefaie, 2020) **Figure 3**

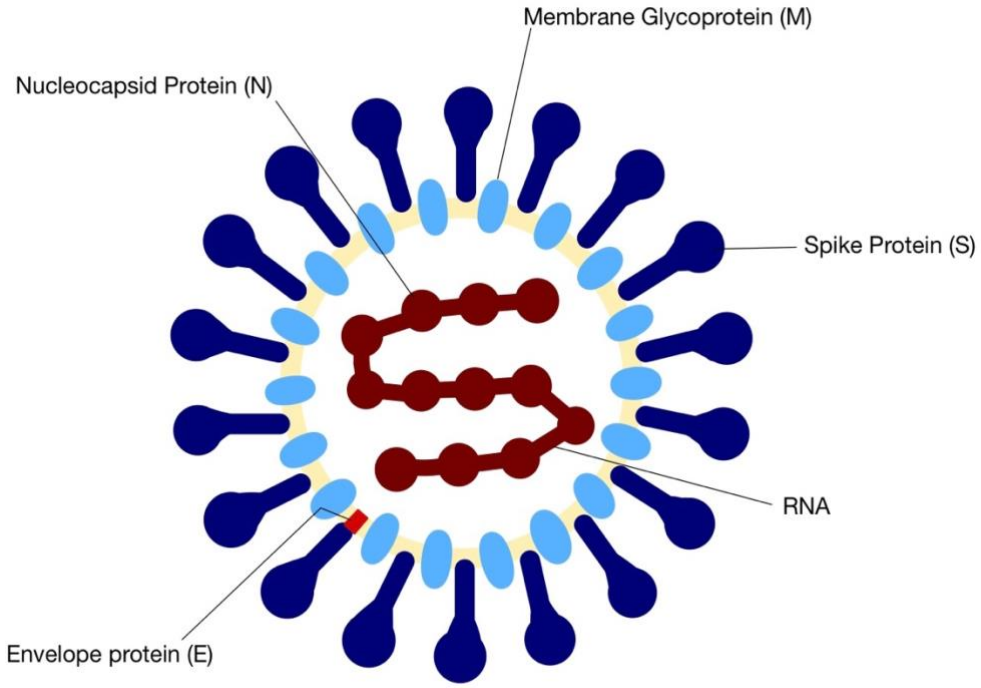

Figure 3 Structure of the Severe Acute Respiratory Syndrome Coronavirus 2 (Sars-CoV-2) Virion*. (N) Nucleocapsid protein, (M) Membrane glycoprotein, (S) Spike protein, (E) Envelope protein. RNA: ribonucleic acid (Mittal* et al.*, 2020)*

1.3.0 Pathogenesis

The RBD domain of SARS-CoV-2' on the S2 protein specifically binds to the human angiotensin-activating-enzyme 2 (hACE2) receptor. The affinity of this RBD for hACE2 significantly surpasses that of SARS-CoV-1 for the same receptor. When the RBD binds to its receptor, it becomes activated. The RBD can transition to a deactivated state to evade an immune response. This state change is facilitated by the top segment of the RBD, either assuming a vertical (activated) or horizontal (deactivated) position. Following the binding of the RBD on the S2 segment to its receptor, S2 and S1 are cleaved by a protease. S2 detaches entirely, while the TMPRRS2 protease primes S1, leading it to undergo a morphological transformation, facilitating its integration with the host cell membrane. (Masters, 2006; Cevik *et al.*, 2020; Shang *et al.*, 2020)

Inside the cell, the RNA (+sense) behaves similarly to mRNA. It gets translated into pp1a and pp1b proteins. These large polyproteins undergo proteolysis, resulting in 16 non-structural proteins (nsps). These nsps constitute the replicase-transcriptase complex, which transcribes the RNA into sub genomes. The positive-sense sub-genome is subsequently translated into structural proteins like E, S, M, and N. The Golgi apparatus orchestrates the assembly of these structural proteins, forming the new virion. Concurrently, other segments of the positive-sense sub-genome undergo transcription and replication to produce the new RNA genome. This genome is then bound by the Nucleocapsid protein, organizing it in a structure reminiscent of a pearl chain. (Masters, 2006; Shang *et al.*, 2020)

1.4.0 Transmission and Epidemiology

The virus is believed to have originated from the Huanan seafood market in Wuhan, China. The outbreak pattern indicates that the market may have been the epicenter of the zoonotic disease's initial spread, though this hasn't been definitively confirmed. (Worobey *et al.*, 2022) Another hypothesis proposes the possibility of a research-related laboratory accident leading to the virus's emergence (Harrison and Sachs, 2022). Due to insufficient evidence, both scenarios remain speculative and unconfirmed. While the virus induces respiratory illnesses in humans, it impacts the

gastrointestinal systems of mammals, including calves and piglets (El-Sayed and Kamel, 2021).

Many Wuhan patients displayed similar symptoms between December 9, 2019, and Feburary 2020. The Chinese government excluded influenza and other known coronaviruses as potential causes of the observed viral pneumonia. By January 7th, authorities identified a new strain of CoV as the cause behind the epidemic. Following this, the Chinese New Year celebrations exacerbated the infection rate within the province. Between January 10th and 22nd, 2020, the period saw a significant case spike due to social gatherings and global travel. (Sohrabi *et al.*, 2020)

Merely 23 days after the SARS-CoV-2 announcement, the WHO declared a public health emergency in response to the virus's rapid proliferation. (Sohrabi *et al.*, 2020)

1.5.0 Acute COVID-19

1.5.1 Symptomatic Pattern

According to the Robert Koch Institute in Germany, the median incubation period is 5-6 days but can extend up to 14 days. The symptoms largely overlap with other respiratory diseases, necessitating differential diagnosis. Initial symptoms commonly comprise fever, cough, olfactory and gustatory dysfunctions, sore throat, and dyspnoea. Often, patients manifest typical symptoms like fever and cough 1-2 days after exhibiting cold-like precursor symptoms. Additionally, some patients might experience body aches, nausea, headaches, or apathy. A definitive diagnosis necessitates a positive PCR test result. Without one, other potential conditions should be considered. ((STAKOB), 2023) It's important to note that different virus variants may produce similar symptoms, but their prevalence may vary. For instance, patients infected with the Omicron variant showed a different set of prevalent symptoms than those who contracted the virus before the emergence of this variant**. Figure 4** compares data from a patient cohort before the spread of the Omicron variant to cohort that tested positive to the Omicron variant. (Menni *et al.*, 2022)

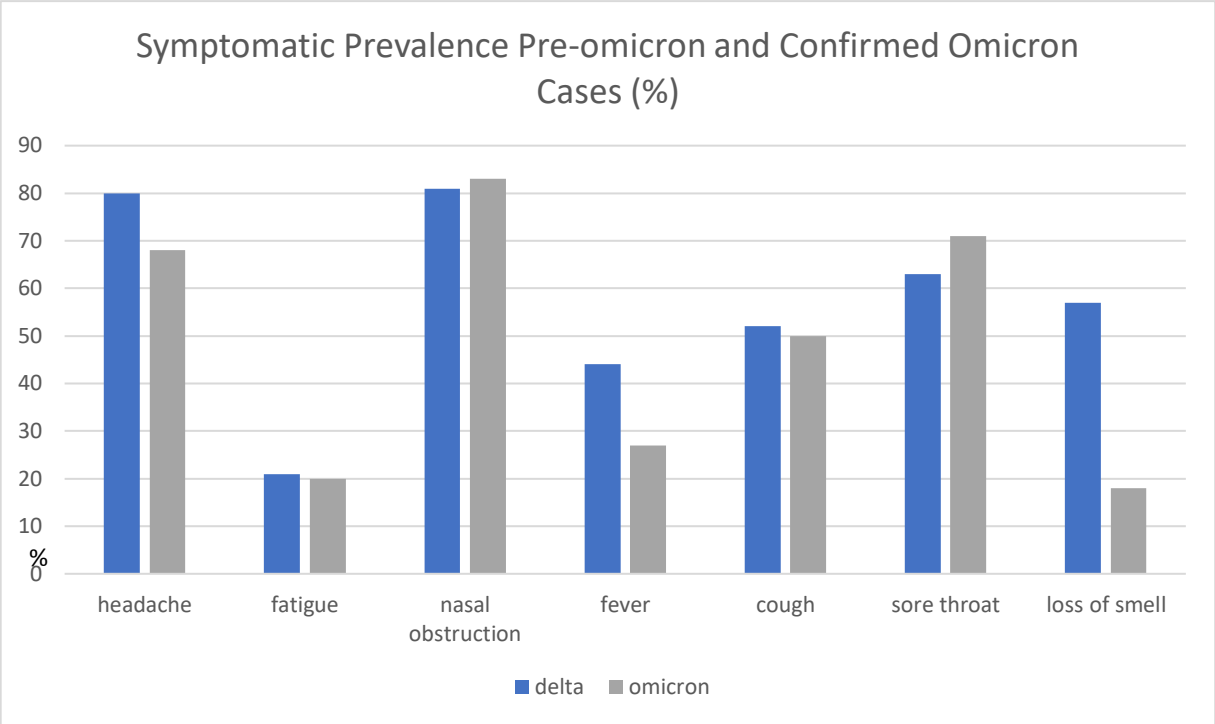

Figure 4 Comparison of the symptomatic distribution in pre-Omicron (blue) and Omicron (grey) cases categorized into their predominant symptoms. The data set is based on a cohort that received 2 vaccinations during the evaluation. *The most common in both was nasal obstruction. (Menni* et al.*, 2022)*

The most common symptom of the Delta variant was nasal obstruction, observed in 81% of cases, closely followed by headaches (80%) and a sore throat (63%). A similar trend is evident in the Omicron cohort, where 83% experienced nasal obstruction, 71% a sore throat, and 68% headaches. The most notable distinction was in the loss of smell, prevalent in 57% of Delta patients, compared to only 17% of Omicron patients. (Menni et al., 2022)

The study generally indicated a lower hospitalization rate during the Omicron wave (1.9%) than the Delta wave (2.6%). As per the study, the symptomatic pattern of the Omicron variant appears to impact the respiratory tract less severely than the Delta variant. Moreover, evidence suggests that the duration of infection is slightly reduced with the Omicron variant compared to the Delta variant. (Menni *et al.*, 2022)

1.5.2 Progression

Most COVID-19 cases are mild to moderate, with a significant portion of asymptomatic courses. However, a smaller fraction is severe or critical. The severity and progression rate are influenced by factors such as the patient's vaccination status, medical history, and the specific variant of the virus contracted. A categorization of severity levels is detailed in **Table 1** below. A patient's medical history is pivotal in predicting the illness's trajectory. Individuals with specific co-morbidities, primarily immune suppression, face a heightened risk of severe outcomes. Many high-risk patients see their conditions deteriorate around days 7-10 post-symptom onset, often accompanied by dyspnoea and hypoxemia. Patients aged 50 and older are at a higher risk, and the presence of multiple pre-existing conditions, such as immune suppression, chronic renal dysfunction, as well as chronic lung and liver diseases, increases the likelihood of severe COVID-19 manifestations. The particular virus variant also plays a role: cases of the Omicron variant have generally necessitated hospitalization less frequently than the Delta variant. ((STAKOB), 2023)

The mortality rate for COVID-19 ranges between 1% and 7%. The predominant cause of death is acute respiratory distress syndrome (ARDS). Its onset is characterized by diffuse alveolar damage (DAD), hyaline membrane formation, desquamation of pneumocytes, and interstitial infiltration. However, not just the death rate but also the long-term effects underline the severity of the illness. (Gagiannis *et al.*, 2020)

1.5.3 Therapy

Therapeutic guidelines should be formulated based on the severity of the disease progression. To make this decision, one must observe the early signs. An increased dyspnea and hypoxemia, coupled with a prolonged fever, can often indicate a potentially severe case. Consequently, the practitioner should initiate early intensive care monitoring. The primary therapeutic approach involves alleviating these symptoms for mild to moderate cases characterized by cough, fever, and headache. Patients are advised to stay home, rest, and avoid contact with others to prevent the spread of the infection. If the symptoms of patients with moderate cases deteriorate,

monitoring should be intensified to ascertain whether the disease is advancing, and a more aggressive therapeutic approach might be required. ((STAKOB), 2023)

Table 1 Classification of the progression severity of acute COVID-19 as defined by the RKI with their matching symptoms. ((STAKOB), 2023) *Polymerase chain reaction (PCR), acute respiratory distress syndrome (ARDS), peripheral capillary oxygen saturation (SpO2)*

Classification	Definition	Symptoms
Asymptomatic	Positive PCR and or antigen test with matching clinical and epidemiological characteristics	none
Mild/moderate	No matching criteria of severe or critical progression	A large variety of symptoms, for example, respiratory symptoms, fever, pneumonia without ventilation, None of the symptoms listed under severe/critical
Severe	Severe Pneumonia	Defined as: Elevated breathing rate of over 30/min SpO2 <90-94%, and radiological indications of pneumonia
Critical	ARDS, sepsis, septic shock, with or without organ failure	Ventilation required or other form of organ support or prescription of vasopressors.

Patients with a more severe course of disease (**Table 1**) should be admitted to the intensive care unit. For such individuals, it is imperative to employ every available measure to support vital parameters, such as ventilation or oxygen supplementation. ((STAKOB), 2023)

Antiviral therapy is advised in these scenarios, encompassing virostatic drugs like polymerase and protease inhibitors that inhibit the SARS-CoV-2 replication process. The goal is to diminish the viral load, thus reducing symptom persistence and severity. This therapy is recommended for patients with high-risk factors and underlying health conditions. Additionally, immune-based therapies utilizing SARS-CoV-2-specific monoclonal antibodies aim to prevent the virus from entering host cells. Yet, this mode of treatment hasn't demonstrated sufficient efficacy and remains secondary.
((STAKOB), 2023)

Early-onset antiviral treatment is advised within five to seven days following the appearance of initial symptoms. However, in some instances, initiating therapy later might be considered. Remdesivir is a frequently utilized antiviral drug, as per RKI guidelines, yet its use is contraindicated for patients with mild to moderate infections. Immune-based therapy is chiefly recommended for patients receiving mechanical ventilation or oxygen supplementation. For instance, Tocilizumab is a monoclonal antibody that obstructs the IL-6 receptor in immune responses, while Dexamethasone, a corticosteroid, is also employed in immune-based therapies. It's important to note that immune-based treatments are typically not advised for patients with mild to moderate disease courses. ((STAKOB), 2023) Corticosteroids have been observed to improve clinical parameters and reduce mortality rates in hospitalized patients needing respiratory support. (WHO Rapid Evidence Appraisal for COVID-19 Therapies (REACT) Working Group *et al.*, 2020)

These drugs likely attenuate the systemic inflammation instigated by COVID-19, which can result in organ failure and lung tissue damage. The RECOVERY trial compared the 28-day mortality rate among 6,425 randomized hospitalized COVID-19 patients: 2,104 received Dexamethasone, and 4,321 got standard care. The findings indicated a notable reduction in mortality among those receiving respiratory aids like ventilation or oxygen supplementation. For those not requiring the aforementioned respiratory aids, there was no observed change in 28-day mortality rates. Moreover, corticosteroid-treated patients typically had a one-day shorter hospital stay than those not treated with Dexamethasone. (RECOVERY Collaborative Group *et al.*, 2021)
Every therapeutic intervention should be individualized based on the patient's medical history and symptomatology. ((STAKOB), 2023)

1.6.0 Post-acute Sequelae of COVID-19 (PASC)

Some patients manifest prolonged health effects following a SARS-CoV-2 infection. The RKI (Robert-Koch-Institute) states that about 40% of all clinically managed patients need extended monitoring and subsequent medical intervention. (Martina, 2020)
Typically, patients recover and are symptom-free between 1 to 4 weeks after the infection. Yet, a long-term study implies that up to 30% of individuals exhibit symptoms post-viral clearance. (Proal and VanElzakker, 2021)

While patients from all severity categories can experience PASC, the age bracket most affected ranges from 36 to 50, typically presenting with mild disease progression without requiring hospitalization. (RECOVERY Collaborative Group *et al.*, 2021)
It's worth noting that various terminologies have been devised to elucidate the persistence of COVID-19 symptoms, further divided based on the infection's timelines and phases. **Table 2** outlines these specific clinical definitions prescribed by the National Institute for Health and Care Excellence. (National Institute for Health and Care Excellence (NICE), 2023)

Table 2 Clinical case definitions to diagnose acute COVID-19 (Coronavirus Disease 2019), ongoing symptomatic of COVID-19, and post-COVID-19, as well as the definition of long-covid as per the guidelines (National Institute for Health and Care Excellence (NICE) et al., 2022). *COVID-19 stands for Coronavirus Disease 2019 (COVID-19)*

Acute COVID-19	**Ongoing symptomatic COVID-19**	**Post-COVID-19 syndrome**
Signs and symptoms of COVID-19 for up to 4 weeks.	Signs and symptoms of COVID-19 from 4 to 12 weeks.	Signs and symptoms develop throughout the infection, lasting more than 12 weeks
The term long COVID is not a clinical case definition per the NICE guidelines; however, it is commonly used to describe signs and symptoms that last throughout ongoing symptomatic COVID-19 in 4-12 weeks and the post-COVID-19 period of 12 weeks and above.		

According to the NICE Guidelines, the most prevalent symptoms included dyspnoea, cough, fatigue, depression, anxiety, cognitive impairment, and difficulty concentrating. The prevalence distribution of the most common symptoms across different time frames is illustrated in **Figure 5**. This data was sourced from three distinct studies. (National Institute for Health and Care Excellence (NICE), 2023)

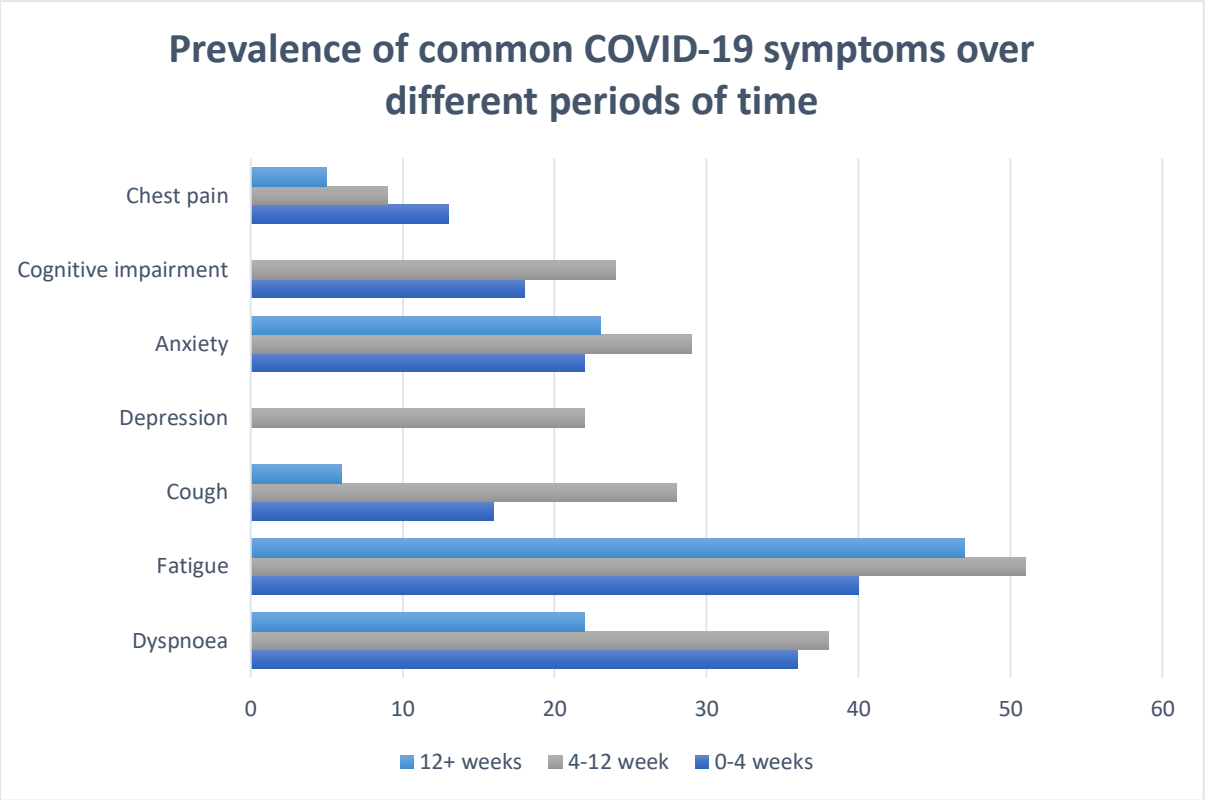

Figure 5 Prevalence of common symptoms of COVID-19 *(Coronavirus Disease 2019) within three different time frames: 0-4 weeks (light blue), 4-12 weeks (grey) and 12+ weeks (dark blue). (National Institute for Health and Care Excellence, 2021)*

Symptoms manifest differently across various periods. For instance, coughing was more prevalent in the initial stages of disease progression (4-12 weeks) at roughly 28%, as opposed to approximately 7% after 12 weeks. In contrast, fatigue was predominant during the 4-12 week span and beyond 12 weeks. Overall, fatigue emerged as the most dominant symptom across all three-time frames, marking its presence during the acute infection phase, ongoing symptomatic phase, and post-COVID phase. This was closely trailed by dyspnoea, which tends to intensify after four weeks, categorizing it as a more prolonged symptom. Two distinct symptom clusters were identified for patients exhibiting symptoms beyond 12 weeks. The "respiratory cluster" encompassed chest pain, dyspnoea, and angina, whereas the "tiredness cluster" consisted of fatigue, dyspnoea, insomnia, and muscle aches. (National Institute for Health and Care Excellence (NICE), 2023)

In addition to subjective symptoms, clinical parameters such as FEV1, TLCO, and VC decrease in spiroergometry. CT results have identified ground-glass opacities (GGO),

consolidations, and subpleural bands. (Trinkmann *et al.*, 2021; Gagiannis *et al.*, 2022). Many cases have shown improvements after steroid treatment. (Myall *et al.*, 2021)

Another study detected restrictive and obstructive changes in lung function tests for PASC-affected patients. Most notably, there was a significant reduction in the lungs' diffusion capacity for carbon monoxide in 39% of the 380 examined individuals. Consequently, patients exhibited subjective and clinical symptoms and experienced clinically noteworthy diminished lung function. (Torres-Castro *et al.*, 2021)

Risk factors potentially precipitating the emergence of persistent symptoms include female gender, hospitalization, advanced age, pre-existing conditions, asthma, and chest pain. (Torres-Castro *et al.*, 2021)

Additionally, patients manifesting over five symptoms within the first month of infection are more susceptible to severe COVID-19 progressions. (Aiyegbusi *et al.*, 2021)

The diverse symptoms result from the virus infiltrating multiple organs via the aforementioned ACE2 receptor. A concise summary of symptoms associated with specific organ damage can be found in **Table 3.** (Crook *et al.*, 2021)

***Table 3 Organ-specific symptoms through the Angiotensin-Converting Enzyme 2 - Receptor pathway after COVID-19 (Coronavirus Disease 2019) infection.* (Crook *et al.*, 2021).**

Organ	Symptom
Kidney	Renal impairment and acute kidney injury
Heart	Angina, Myocardial inflammation, Palpitations, Elevated serum troponin
Brain	Delirium, Fatigue, Sleep deprivation, Depression, Anxiety
Gastrointestinal tract	Diarrhea, Nausea, Sore throat
Blood vessels	Inflammation, Vessel damage, Coagulopathy
Liver	Liver injury

The primary interest lies in the virus's impact on the lungs. In a 2021 study by (Yong, 2021), dyspnea was observed in 43.3% of 143 patients 60 days post-infection. As it is the aim to delineate the defining characteristics of long COVID/PASC, it's evident that its scope is broader than initially presumed. Notably, this condition doesn't solely affect patients with a severe disease course. Multiple studies indicate that many patients,

even those who experienced only mild-to-moderate disease progression, present symptoms consistent with long COVID/PASC. Hence, diverse symptoms affect patients across all age groups and medical backgrounds. (Yong, 2021)
Long-term studies and comprehensive data are essential to grasp its lasting effects. However, the pandemic's magnitude has accelerated global research, significantly boosting the understanding of the subject.

1.7.0 Possible Causes of PASC

A Canadian study found that symptom severity and persistence correlated with levels of ANA and cytokines. (Son *et al.*, 2023) SARS-CoV-2 is associated with superantigens, which have been shown to trigger a cytokine storm through T-cell activation. Under physiological conditions, a Dendritic Cell (DC) presents the pathogenic antigen to the T-lymphocyte. Such lymphocytes only activate if they possess a matching T-cell receptor (TCR) to the major histocompatibility complex (MHC). Upon activation, they undergo clonal expansion. If a DC presents a superantigen, binding occurs outside the TCR, activating an entire subgroup instead of a specific T-cell. This results in a significantly increased concentration of non-specific T-lymphocytes, causing a dysregulated immune response. (Jacobs, 2021)
Identifying if the cause is a hyperactive immune reaction or an ongoing infection since both are indications for different treatment approaches. Fighting viral presence with interleukins or antivirals is advised in an ongoing infection. (Jacobs, 2021) In a hyperactive immune reaction, guidelines suggest decreasing the immune response using corticosteroids, as suggested in the RECOVERY trial above. (Jacobs, 2021; RECOVERY Collaborative Group *et al.*, 2021)
While the primary cause of PASC remains unclear, evidence suggests that a malfunctioning CD8+-cell response may instigate chronic inflammation, impairing lung function in SARS-CoV-2 survivors. A study indicated an elevated presence of memory B and T-cells within lung tissues of COVID-19 patients. Specifically, higher concentrations of CD8+ cells correlated with decreased lung function. Although CD8+ T-cells are pivotal in combatting viruses, this study identified specific CD8+ T-cell subgroups with pathogenic characteristics that harm lung tissue. It's worth considering whether the T-cell response in the respiratory system might be a primary factor behind pulmonary PASC symptoms. (Cheon *et al.*, 2021)

Another investigation explored whether anti-nuclear/extractable-nuclear antibodies (ANAs/ENAs) remain detectable in convalescents a year after virus clearance and if this correlates with PASC manifestations. Antibody levels were assessed six days and two months post-infection. The study discovered that, even after 12 months, ANA/ENA levels, accompanied by pro-inflammatory cytokines like TNF-α or C-reactive protein, remained high in cases of PASC. Patients who reported at least one PASC symptom a year after recovery exhibited persistently elevated ANA/ENA levels. Specific antibodies, notably anti-U1-snRNP and anti-SS-B/La, were closely associated with symptoms like dyspnea and fatigue. The pronounced correlation between TNF-α and ANA/ENAs and their predictive capability regarding PASC symptom persistence in previously healthy individuals suggests a role of autoimmunity in symptom endurance post-viral clearance. (Son *et al.*, 2023)

One study noted viral shedding in the gastrointestinal tract (GIT) 33 days following a negative PCR test. (Widders, Broom and Broom, 2020) There was also evidence of viral fragment persistence in various organs, such as the brain, eyes, and heart, months after infection. (Merad *et al.*, 2022)

The presence of these viral remnants might underpin elevated cytokine concentrations. Another study posited that specific antibodies might facilitate the retention of these viral fragments. (Merad *et al.*, 2022)

1.8.0 Post-viral Pulmonary Diseases

PASC shares many symptomatic patterns with other respiratory diseases that follow viral respiratory infections, such as asthma, ARDS, and pneumonia. (Hansbro *et al.*, 2008; Frickmann *et al.*, 2012)

Therefore, differentiation and comparison are essential. Some results might overlap with other respiratory illnesses from various etiologies when evaluating the data. Consequently, I will provide an overview of the most common post-viral pulmonary diseases as well as complications from infectious disease in the lung

1.8.1 Pneumonia

Pneumonia refers to the inflammation of lung tissue. Various bacteria, fungi, or viruses, including adenovirus, influenza, and SARS-CoV-2, commonly cause it. When induced by viruses in patients without a relevant medical history or co-morbidities, it can be classified as simple viral pneumonia. (Kim *et al.*, 2002)

Symptoms often include cough, chest pain, and shortness of breath. Pneumonia frequently necessitates hospitalization and proves fatal in 10% of cases. (Lungeninformationsdienst, 2020). Co-morbidities and advanced age can escalate the severity. Viruses are believed to account for up to 44% of all pneumonia cases. This estimation is a recent development; previously, the numbers were lower due to false-negative nasopharyngeal PCR testing. Many guidelines suggest radiological imaging and computed tomography when the diagnosis isn't evident. (Dueck *et al.*, 2021) Radiological findings might indicate ground-glass opacities, occasional reticular areas, and consolidation. CT scans often depict consolidation, ground-glass attenuation with lobular distribution, or intralobular septa. It's crucial to remember that imaging can widely vary, which reflects the diverse histopathologic patterns in pneumonia, encompassing DAD, infiltration, and interalveolar extravasate (Kim *et al.*, 2002). Bacterial superinfections (e.g., Staphylococcus spp. and Streptococcus spp.) and fungal superinfections (e.g., Aspergillus spp.) are potential complications of viral pneumonia. The immunosuppression seen during pneumonia treatments can create an environment conducive to these superinfections. While bacterial infections are more prevalent, fungal infections are more lethal. (Obar and Shepardson, 2023)

1.8.2 Acute Respiratory Distress Syndrome (ARDS)

The defining feature of ARDS is the buildup of capillary exudate, cellular debris, and inflammatory cells within the alveolar spaces, leading to formation of hyaline membranes, further impeding gas exchange. Consequently, ARDS's histopathologic counterpart is often called diffuse alveolar damage (DAD) or hyaline membrane disease. The inflammatory processes degrade the surfactant, reducing surface tension and potential alveolar sac collapse. Symptoms commonly include dyspnea, increased respiratory rate, fever, chest pain, cough, lung crackles, and tachycardia. Damage to the alveoli can instigate structural changes, possibly culminating in lasting lung function impairment like fibrosis. While ARDS can emerge at any age, it's predominantly

triggered by lung injuries, sepsis, pancreatitis, or viral infections. (National Heart, Lung, and Blood Institute, 2023)

Viral infections of the respiratory system are a frequent cause of ARDS. Inflammatory processes underpin roughly half of all ARDS instances. Pneumonia, sepsis, and certain respiratory viruses, including Influenza, Adenovirus, Human Metapneumovirus, and Coronaviruses, are common inflammatory causes. (Luyt *et al.*, 2011) ARDS can be severe but potentially reversible due to viral infection. Therefore, clinicians should conduct comprehensive microbiological tests for an accurate and timely diagnosis, incorporating urine samples, serological tests, blood cultures, fiber-optic BAL, and lavage. CT scans commonly reveal three primary manifestations, which often coexist: regions of consolidation, ground-glass opacity, and areas with regular ventilation. Ultrasonography also plays a valuable role in diagnostics (Papazian *et al.*, 2016). ARDS treatment alleviates hypoxemia and addresses the root cause to prevent alveolar structural alterations. Oxygen therapy is the primary treatment approach, with invasive ventilation recommended for more severe cases. Blood transfusions might be advised to augment reduced hemoglobin levels. Physical therapy and intravenous fluid administration are conventional practices. (National Heart, Lung, and Blood Institute, 2023)

1.8.3 Asthma

Asthma is characterized by the constriction of the airways, resulting in an obstructive breathing pattern. This is primarily caused by a hyperactive inflammatory immune response in the airway walls. Increased mucus production, hyperreactivity of bronchial muscles, tissue edema, and ongoing inflammatory processes create asthma's characteristic symptoms. Common presentations include dyspnea, coughing, and chest pain. While many of these symptoms can be treated and the obstruction reversed, chronic inflammation can cause tissue restructuring, leading to permanent airway obstruction. (Padem and Saltoun, 2019; Hammad and Lambrecht, 2021) Causes range from allergic reactions and chronic exposure to toxins, like smoking, to viral infections. Asthma can be broadly classified into allergic and non-allergic types. Early-onset asthma in children is mainly allergic and associated with T helper 2 (Th2) cells. These cells mediate various allergic reactions and can be triggered by common allergens like house dust or pollen. In this context, Th2 cells activate cytokines in the airway tissue, increasing mucus and IgE secretion.

In contrast, non-allergic asthma typically affects older patients and is often associated with smokers, the obese, and the elderly. It's worth noting that children with early-onset asthma who frequently experience respiratory infections, especially of viral origin, often face a more severe progression. Such diseases in these children are more likely to persist. Various factors can exacerbate asthma, including pollution, allergens, and cold air. However, respiratory viruses play a significant role, mainly because they target inflamed lung tissue. This pre-existing inflammation compromises the immune response to the virus, prolonging the symptoms and the inflammation. Elevated IgE and blood eosinophil levels, coupled with low-type IFN concentrations, can result in more severe exacerbations. Conversely, a high concentration of Th2 cells in the airway wall's epithelial tissue facilitates faster viral clearance, ensuring a better prognosis and reduced symptom duration (Hammad and Lambrecht, 2021). The NICE guidelines identify clinical manifestations such as wheezing, dyspnea, coughing, specific exacerbating substances, and family history. A polyphonic wheeze during expiration is particularly indicative of asthma. However, as a diagnosis should not solely depend on clinical observations, the NICE guidelines recommend further testing. Standard diagnostic methods include spirometric parameters like FEV1, forced vital capacity (FVC), and the FEV1/FVC ratio, offering insight into significant airway function. Monitoring peak flow variability fractional exhaled nitric oxide testing and direct bronchial challenges using histamine or methacholine are also suggested. The exact diagnostic approach depends on the patient's age, medical history, and symptoms. Treatment varies per patient but typically involves a combination of drugs such as short-acting beta2 agonists (SABA), inhaled corticosteroids, leukotriene receptor antagonists (LTRA), and long-acting beta2 agonists (LABA). (National Institute for Health and Care Excellence (NICE), 2023)

1.8.4 Bronchitis

Viruses, including rhinovirus, enterovirus, coronavirus, and Influenza A or B, cause most bronchitis cases. The hallmark symptom is a cough, which may accompany dyspnea, nasal congestion, fever, and headaches. Recovery typically takes up to three weeks. Since bronchitis's differential diagnosis encompasses a wide range of severe illnesses like asthma, pneumonia, or COPD, clinicians should employ radiological

imaging to exclude these conditions. Treatment is primarily supportive, with antibiotics typically not recommended. (Kinkade and Long, 2016)

1.8.5 Bronchiolitis

For bronchiolitis, the framework proposed by Jay H. Ryu can be referenced, summarized in **Table 4**. It's worth noting that many disorders listed in **Table 4** can also manifest in the context of connective tissue diseases. (Ryu, Myers and Swensen, 2003)

Table 4 Classification of bronchial abnormalities as proposed by Ryu (Ryu, Myers and Swensen, 2003). Categorized into three classifications with the matching clinical manifestations

1 Primary bronchiolar disorder the etiology originates in the bronchioles	**2 Parenchymal disorder** impact the bronchiolar function	**3 Bronchiolar involvement** in large airway diseases
-Constrictive bronchiolitis (obliterative bronchiolitis, bronchiolitis obliterans) -Acute bronchiolitis -Diffuse panbronchiolitis -Respiratory bronchiolitis -Mineral dust airway disease follicular bronchiolitis	-hypersensitivity pneumonitis - respiratory bronchiolitis Associated interstitial Lung disease - cryptogenic organizing pneumonia (idiopathic bronchiolitis obliterans organizing pneumonia) - pulmonary Langerhans' Cell histiocytosis.	- bronchiectasis - asthma - chronic obstructive pulmonary disease

Bronchiolitis targets the bronchioles (with a radius of 1mm or less) and entails inflammation that can lead to fibrotic remodeling. It's imperative to recognize that the extent and severity of tissue damage can differ. This condition is the most common disease diagnosed in the small airways. In young children, bronchiolitis is primarily due to viral causes (Ryu *et al.*, 2020)

However, In adults, its causes are diverse and categorized into various subtypes, such as obliterative, respiratory, and acute bronchiolitis, as seen in **Table 4** (Ryu *et al.*, 2020). CT imaging proves beneficial in diagnosis. Characteristic diagnostic features of bronchiolitis include bronchiectasis, wall thickening from inflammatory or fibrotic processes, and luminal narrowing, visible as peripheral markers in imaging. Other less definitive signs include air trapping, which can produce a mosaic pattern in HRCT, indicative of areas of low lung attenuation. An obstructive pattern, marked by impaired exhalation due to inflamed airways, is characteristic of several bronchiolitis subtypes. Constrictive bronchiolitis is a prime example, with fibrotic deposits causing bronchiole narrowing or even total obstruction. (Ryu *et al.*, 2020).

Bronchiolitis can also emerge post lung, heart, or bone marrow transplants. Strikingly, up to 65% of patients experience constrictive bronchiolitis within five years post-lung transplant, becoming the leading mortality cause in this context. This chronic constrictive bronchiolitis in transplant recipients is termed bronchiolitis obliterans syndrome. However, obliterative bronchiolitis is not limited to transplant recipients or those with connective tissue diseases. It is frequently observed in post-viral infections in adults. Adenovirus and influenza infections, for instance, can precipitate acute bronchiolitis in adults. It's crucial to realize that lung structural alterations might manifest during acute infection and emerge after viral clearance (Ryu *et al.*, 2020).

While symptomatic displays might differ based on the infection type, a general agreement exists regarding specific histological presentations across subgroups. Evidence suggests that profibrotic cytokines, instrumental in fibrosis development, arise from virus-induced inflammation and reduced airway blood flow (Ryu *et al.*, 2020). This bronchiolitis form is typically chronic, resulting in declining lung function, which can be lethal. Since bronchioles are the primary sites affected, obliterative bronchiolitis can be categorized as group one in Ryu's classification scheme **(Table 4**) (Ryu, Myers and Swensen, 2003).

1.9.0 Interstitial Pneumonia with Autoimmune Features (IPAF)

IPAF is a newly coined term to describe patients with interstitial lung disease caused by an autoimmune condition that doesn't fall under the category of rheumatoid connective tissue diseases (CTD), such as rheumatoid arthritis or Sjögren’s Syndrome.

The criteria for this new term are summarized in **Table 5**. (Płóciniczak, Goździk-Spychalska and Batura-Gabryel, 2017)

Table 5 Criteria for the new proposition of the term Interstitial Pneumonia with Autoimmune Features (IPAF) in the clinical, serologic and morphologic domain (Płóciniczak, Goździk-Spychalska and Batura-Gabryel, 2017)*. Antinuclear antibodies (ANA), High-resolution computer tomography (HRCT), non-specific interstitial pneumonia (NSIP), anti-cyclic citrullinated peptide antibodies (Anti-CCP), anti-double-stranded DNA (Anti-dsDNA)*

Clinical domain	Serological domain	Morphologic domain
-distal fissuring -digital tip ulceration -Inflammatory arthritis or polyarticular morning joint stiffness >60 mins -Palmar telangiectasia -Unexplained digital oedema -Gottron's sign	-ANA ≥1:320 titre, diffuse, speckled, homogeneous patterns *or* -ANA nucleolar pattern (any titre) *or* -ANA centromere pattern (any titre) -Rheumatoid factor ≥2× upper limit of normal -Anti-CCP, Anti-dsDNA, Anti-Ro, Anti-ribonucleoprotein, Anti-Smith, Anti-topoisomerase	-Suggestive radiology patterns by HRCT (e.g. NSIP/OP) -Histopathology patterns or features by surgical lung biopsy (e.g. NSIP/OP) -Multicompartment involvement (in addition to interstitial pneumonia) such as Unexplained pleural effusion/thickening

A prior study investigated patients experiencing respiratory difficulties following a mild COVID-19 infection. Most patients displayed reduced oxygen pulse, lymphocytosis, increased LAV, organized pneumonia, and fibrin deposition. The combined radiological and clinical findings met the criteria for IPAF classification. Since interstitial collagen deposition was also observed, it's crucial to closely monitor these cases to detect any potential development of fibrosis in mild COVID-19 PASC patients. (Steinestel *et al.*, 2021)

1.9.1 The Objective

The onset of the global pandemic in 2020 was attributed to the novel respiratory virus, SARS-CoV-2 (Shanmugam *et al.*, 2020). Its symptoms range from common manifestations like coughing, fever, and fatigue to more severe effects like cognitive impairment and anxiety (National Institute for Health and Care Excellence (NICE), 2023). Clinically, three definitions pertain to the infection's duration and symptoms: acute COVID-19 (symptoms lasting up to four weeks), ongoing symptomatic COVID-19 (symptoms from 4 to 12 weeks), and post-COVID-19 syndrome (symptoms extending beyond 12 weeks). (National Institute for Health and Care Excellence (NICE), 2023) The most frequent long-term (12+ weeks) complications include fatigue, dyspnea, and anxiety. (National Institute for Health and Care Excellence (NICE), 2023) Theories behind these persistent symptoms encompass continuous viral presence, resulting in ongoing inflammation and an unsuccessful autoimmune response. (Jacobs, 2021)

Various respiratory viruses lead to acute and post-viral conditions, such as pneumonia, ARDS, asthma, bronchitis, and bronchiolitis. Given that some characteristics of these diseases overlap with the reported PASC manifestations, it becomes vital to delineate this pathology and compare its lung involvement patterns with other conditions.

The main objective of this study was to investigate the radiological, clinical, histopathological, and serological features of pulmonary PASC. A final cohort of 51 PASC patients consented to various diagnostic procedures such as radiological imaging, serology, and bronchoscopy was identified after thorough examination and exclusion of other causes of respiratory distress. High-resolution computed tomography (HR-CT), biopsies (n=51), and/or bronchoalveolar lavage (n=18) were performed to assess PASC-ILD. Autopsy samples (n=15) served as a comparison group. The comprehensive analysis included ANA/ANCA/ENA screenings for serology, SARS-CoV-2 detection through FISH and RNA extraction, and spiroergometry to measure various parameters during incremental training phases. Bronchoscopy involved anesthesia and tissue sampling for extensive analyses, including histology, immunohistochemistry, macrophage phenotyping, and electron microscopy. A control group of 15 pre-pandemic autopsy samples was also included. The comprehensive approach of this study aims to elucidate the pulmonary manifestations of the post-acute consequences of SARS-CoV-2 infection.

2.0.0 Material and Methods

2.1.0 Patients and Diagnostics Workup

The present study included n=66 patients with a history of RT-PCR-confirmed SARS-CoV-2 infection and persistent pulmonary symptoms. All were unvaccinated at the time of the SARS-CoV-2 infection. The baseline diagnostic workup included clinical history, current and previous medication, allergies, physical examinations, ANA/ANCA/ENA screenings, and spiroergometry. After multidisciplinary discussions, bronchoscopy with transbronchial biopsy to assess PASC-ILD was performed in n=51 definite cohort patients. Patients had given written informed consent to routine diagnostic procedures (serology, bronchoscopy, imaging) and the science data and tissue samples in the present study. The control cohort consisted of 15 pre-pandemic autopsy samples. This project was approved by the local ethics committee of the University of Ulm (ref. no. 129-20 and 331/20) and conducted per the Declaration of Helsinki (Gagiannis *et al.*, 2023).

2.2.0 Serology

Initial screenings for ANA and ANCA (p-ANCA, c-ANCA, x-ANCA, Anti-PR3, Anti-MPO) were performed by IIF using patient sera on Hep-2 cells and primate liver tissue slides (ANA) as well as ethanol- and formol-fixed granulocytes and purified PR-3 and MPO antigens (ANCA) on glass slides (Euroimmun AG, Lübeck, Germany) according to the manufacturer's protocols. In all cases, presence of specific anti-ENA autoantibodies (anti-Sm, anti-SS-A/Ro, anti-SS-B/La, anti-Scl-70, anti-centromere, anti-Jo1, anti-Mi-2, anti-U1-RNP, anti-Ro-52, anti-PM-Scl, anti-CNP B, anti-PCNA, anti-dsDNA, anti-nucleosome, anti-histone, anti-ribosomal P-protein, anti-AMA-M2) was assessed by semiquantitative immunoblot (Anti-ENA Profile 3; Euroimmun AG, Lübeck, Germany) irrespective of the initial screening result. Following previously published guidelines, ANA titers ≥1:320 with or without positive ENA immunoblot or ANA titers of 1:100 with positive ENA immunoblot were regarded as positive. Laboratory testing was performed by investigators who were blinded to patient status, and in cases with unclear/borderline results in either ANA screening or ENA subtyping, tests were repeated on a new sample, and an external reference laboratory verified

results. The quality and reliability of ANA/ANCA/ENA testing in the institution have been evaluated through regular interlaboratory ring trials.

2.3.0 Histology and Sars-CoV-2 Detection

For SARS-Cov-2 fluorescence in situ hybridization (FISH), paraformaldehyde-fixed, paraffin-embedded 1µm section of transbronchial biopsies (TBBs) and lung autopsy material (positive controls) were deparaffinized followed by dehydration with 100% ethanol. FISH was performed with the RNAscope® Multiplex Fluorescent Reagent Kit v2 assay (Advanced Cell Diagnostics, Inc.) according to the manufacturer's instructions. Briefly, a heat-induced target retrieval step followed by protease was performed. Afterwards sections were incubated with the following RNAscope® Probe - VnCoV2019-S (#848561-C1), -V-nCoV2019-S-sense (#845701-C1), -Hs-ACE2-C2 (#848151-C2) and -Hs-TMPRSS2- C2 (#470341-C2). After the amplifier steps, the fluorophores OpalTM 570 and 650 (PerkinElmer Life and Analytical Sciences) were applied to the tissues incubated with C1 and C2 probes, respectively. Finally, nuclei were stained with DAPI and the slides were mounted with ProLongTM Gold antifade reagent (Invitrogen). Sections were analyzed with Zeiss Axio Imager 2 and image analysis software (ZEN 3.0 blue edition). SARS-CoV-2 RNA was extracted using Maxwell® 16 FFPE Plus Tissue LEV DNA Purification KIT (Promega) on Maxwell® 16 IVD Instrument (Promega). Using TaqMan® 2019-nCoV kit (ThermoFisher), the detection of SARS-CoV-2 E-gene was performed according to the manufacturer's instructions. (Gagiannis *et al.*, 2023)

2.4.0 Spiroergometry

2.4.1 Devices

The patient's respiratory flow was measured using the spiroergometric device of the Quark measuring unit manufactured by COSMED, based in Rome, Italy. The Quark unit determines the patient's athletic output through a panel on the Ergometer LC 6 (Monark, Varberg, Sweden). On the bike, the subject's breath is limited through a mouthpiece. Said mouthpiece allows the surrounding air intake through a vent with each breath. The nose is blocked with a clip throughout the entire period of exercise.

A pneumotachograph measures airflow to record the flow velocity of the breath. Using the gas analysis module, an additional tube is attached to the mouthpiece to measure the expiratory breath's respiratory CO_2, O_2, and end-tidal CO_2 concentrations.
The Quark unit records the measurements in one one-second intervals. Furthermore, other parameters such as VO_{2max}, VE/VEO_2 a, and $VE/VECO_2$ can be calculated. All data can be viewed on the monitor and is saved on the computer's hard drive during and after the examination. If required, all outcomes can be printed on the adjacent printer.
Final parameters were then averaged within twenty-second intervals.
According to the operation manual, the devices were calibrated upon volume and gas analytics daily before their primary use.
Oxygen saturation levels and the pulse were measured using a pulse oximeter (Quark/K4b2 Oximeter Xpod Prob) as a clip placed at the tip of the patient's finger. To measure ECG parameters, the PC PC-based-Channel electrocardiograph ECGpro CardioPart 12 Blue-s CPET-Set (AMEDTEC, Aue, Germany) automatically records and interprets data before wirelessly transferring said results to the monitor. Finally, the software could summarize the key data points and highlight examination highlights pressure measurements by applying the Riva Rocci method using an upper arm cuff and the Korotkow sounds. The cuff's circumference could range from 25-31 cm to cater to patients of all sizes.
To determine the blood gas levels, samples were taken from the earlobe. Twenty minutes before the examination, Finalgon® was applied to the earlobe. Finalgon®, containing Nonivamide and Nicoboxil, causes vessel dilation and significantly increases blood flow.
The desired area was pecked with a needle, and small amounts of blood were transferred into a heparin-laced glass tube to retard the coagulation process. The device used to measure the blood gas levels is ABL90 Flex plus (Radiometer, Copenhagen, Denmark).

2.4.2 Procedure

The examination proceeded within the following guidelines. The patient was placed on the ergometric bike in a slightly forward-leaning position. The subject's upper body was

bare, and the 12-channel electrodes for the ECG, the oximeter finger clip, and the arm cuff of the blood pressure monitor were applied.
The seat height was adapted so the subject's knee was bent when paddling.
After guiding them through the procedure, the nose clip and mouthpiece were set in place. The patient was then instructed to exercise until their subjective maximum capacity. Once the maximum is reached, this should be communicated with a hand sign seconds before the termination of the exercise.
Once an accurate ECG was recorded, the examination began with a rest phase of two minutes. During this time, the subject had the chance to get acquainted with breathing through the mouthpiece. Consecutively, the blood pressure, blood oxygen levels, pulse, and blood sample from the ear lobes were taken. The results were then recorded as the baseline values.
The resistance of the ergometric bike started at 25 Watts and increased by another 15 Watts every minute. The aim was to paddle at a frequency of 50 to 60 turns per minute. The twelve-channel ECG that was continuously monitored could be viewed on the computer monitor. The scale was equivalent to a 50mm paper feed, therefore 50mm/s. The data was summarized and highlighted the most prominent data points of the ECG. The QRS complexes could then be printed to view in analog form.
After the subjects had ended the period of physical exercise because they had reached their maximum subjective capacity, several parameters were deducted immediately. These parameters included the blood pressure, pulse, ECG with a 50mm paper feed (50mm/s), collection of capillary blood from the earlobe for the blood gas analysis, and blood saturation levels. After collecting all the data, the patients could terminate the physical exercise, and the post-observation period began. However, the subjects were still required to breathe through the mouthpiece for another eight minutes, during which further values using the ECG, the oximeter, and the blood pressure monitor were recorded. These results were obtained within the resting period's first, third, fifth, and eighth minutes. Another probe of capillary blood was attained in the third and eighth minute from the earlobe.
Provided the patient felt comfortable and well, they could step off the bike at the end of the examination. The examiner and subject could decide to stop the procedure at any given time due to the objective reasons in the following abstract.

2.4.3 Termination Criteria

The termination criteria on the part of the patient and the examiner are listed as follows:

Termination criteria on behalf of the examiner:

- ECG variations under physical strain
  - Repolarization disturbances
  - Cardiac arrhythmia: increased extrasystoles, short salvos, atrial fibrillation, atrial flutter, ventricular tachycardia
  - New blockages include Atrioventricular Blocks and left bundle branch block of the II. or III. Degree
- Systolic blood pressure of 230mmHg and above, and/or a diastolic blood pressure of 120mmHg or above.
- Heart rate below ten bpm
- Drastic increase in blood pressure (10mmHg per resistance increase)
- Diminishing blood pressure

Termination criteria on behalf of the patient:

- Angina Pectoris
- Intolerable dyspnoea
- Nausea
- Joint or muscle discomfort or pain
- Fear or phobia
- Exhaustion

2.4.4 Measured and Calculated Parameters of Spiroergometry

The following data was directly measured or calculated by the spiroergometric device and integrated into the statistic evaluation. **Table 6**

Table 6 Measured parameters during Spiroergometry. *Electrocardiogram (ECG) Carbon dioxide (CO_2), Oxygen (O_2), Volume of Oxygen (VO_2), Volume of Carbon dioxide (VCO_2), Minute Ventilation (Mv), Ventilation (VE)*

Measured parameters	Calculated parameters
• Height • Weight • Air pressure • Humidity • Heart rate • Blood pressure • ECG • Respiratory rate • Load level in Watts • Time • Blood gas analysis • Volume flow of breath • Respiratory gas concentration (O_2 and CO_2)	• Body surface area • Tidal volume or respiratory volume • Minute Ventilation (M_V) • Oxygen absorption (VO_2) • Carbon dioxide absorption (VCO_2) • End-tidal O_2- and CO_2 partial pressure (PetCO2 & PetCO2) • Highest oxygen absorption (Peak VO_2) • Respiratory equivalent for O_2- &CO_2 (VE/VO2 & VE/VCO2) • Respiratory Exchange ratio (RER)

2.5.0 Radiology

The thorax's computed tomography (CT) scans were obtained using the third-generation DECT Siemens Somatom Force (Siemens Healthineers, Forchheim, Germany) as a multislice-spiral CT in complete dose technique. (Qual. Ref. kV: Sn 100, Qual. Ref. mAs: 600). The collimation was 192 x 0.6 mm, utilizing a tin prefilter at 100 to 150 kV. The rotation time was 0.25 seconds, and the scanning interval was 1,25 seconds. The CT was administered while the patient was inhaling. Before the procedure began, the patients were informed of all risks and side effects.

The scans were then automatically evaluated and numerically interpreted using the software “syngo.via”, version VB 40 (Siemens Healthineers, Forchheim, Germany). The software used the program “CT Pulmo 3D” to retrieve the numeric values.

The relevant measured parameters were the volume (ml), relative volume (%), average lung density in Hounsfield units (HU), SA (HU), full width at half maximum (FWHM), low attenuation volume (LAV %), high attenuation volume (HAV %).

These parameters were obtained by following these criteria:

Layer thickness of 0,0.75m, increment 0.5 mm, reconstruction using a medium-soft kernel BR 40, iterative reconstruction: admire stage 3, display in soft tissue window (C45 W 340).

The lower threshold was at (LAV) -950 HU, and the upper threshold was at (HAV)-200 HU.

2.6.0 Bronchoscopy and Lung Sampling

For the bronchoscopy and bronchoalveolar lavage, patients were administered 1,5 mg Midazolam, 120mg Propofol, 500 ml Normofundin, Arcoin2% 2x5ml anesthetic, and Oxybuprocain (Novesine) 1%. The Bronchoscope, BF-TH190 (Olympus, Tokyo, Japan), was orally inserted into the larynx. The Glottis and vocal cords were passed. The process continued with a protective intubation using a 7,5 intervention tube. After following the bronchus and positioning the bronchoscope, bronchioalveolar lavage followed. The lavage was performed within segment five of the right lung. A saline solution was instilled into the desired segment of the lung. After it has been recovered,

lavage solution was sent to 1. cell quantification (Gärtner laboratory, Ravensburg), 2. microbial analysis (fungi/bacteria) (Institute of Microbiology University Hospital Ulm), and 3. cytokine profiling (Dept. of Molecular Virology, University of Ulm). Following the lavage, transbronchial tissue samples were taken from segments 8-10 of the right lung. One sample was stored in a 4% buffered aqueous formaldehyde solution (formalin), while the second sample was immersed in 4% paraformaldehyde in 0.1M PBS (pH 7.4) for transmission electron microscopy. While the classic FFPE sample for light microscopy and (immuno)histochemistry was processed by the Institute of Pathology at the military hospital Ulm, the EM analyses were performed by Prof. Bloch at the German Sports University, Cologne.

2.6.1 Histology and Immunohistochemistry

Transbronchial biopsies in the form of lung tissue specimens were fixated in 4% buffered formalin and later embedded in paraffin (FFPE). The autopsy control samples were derived from the FFPE archive of the Institute of Pathology of the Bundeswehrkrankenhaus Ulm. 4µm-thick paraffin slides were stained with hematoxylin-eosin (HE), Phosphotungstic-Acid-Hematoxylin (PTAH), Elastica-van-Gieson (EvG), and Masson-Goldner (MG). Light microscopy was performed on a Leica DM6000 light microscope (Leica, Wetzlar, Germany) with digital image acquisition using the Diskus Mikroskopische Diskussion imaging software (Diskus, Königswinter, Germany).

Prediluted (ready-to-use) rabbit monoclonal antibodies against CD4 (SP35) and CD8 (SP239) were obtained in form from Roche/Ventana Medical Systems (Tucson, USA) and stained on a BenchMark Autostainer (Ventana Medical Systems, Tucson, USA). Finally, sections were washed in water, lightly counterstained with hematoxylin, dehydrated, and mounted. Omitting the primary antibody from the immunohistochemical procedure and replacing it with an antibody diluent acted as the negative control.

2.6.2 Staining Macrophage Panel

Slides underwent antigen retrieval in citrate buffer (EnVision flex target retrieval solution low pH, from Agilent: K8005) using the pT-Link module (Agilent, Santa Clara, USA). After fixation in 4% formalin for 10 min, slides were washed, and blocking was performed with H2O2 (DAKO REAL PEROXIDASE-BLOCKING SOLUTION, Agilent, Santa Clara, USA: S2023) followed by 30 min incubation with antibody diluent (DAKO REAL ANTIBODY DILUENT, Agilent, Santa Clara, USA: S2022). Immunofluorescence multiplex staining was performed with Opal 7-Color Manual IHC Kit (AKOYA Biosciences, Menlo-Park, USA: NEL811001KT). The slides were incubated for 1 hour with primary antibodies: CD68 (Agilent, Santa Clara, USA: M0876), CD163 (Cell Marque: 163M-17), S100A9 (Abcam: ab63818) and CD16 (Santa Cruz Biotechnology, Dallas, USA: DJ130c), followed by incubation with EnVision FLEX HRP (Agilent, Santa Clara: DM802) and visualized with Opal 690 TSA Plus, using Opal 650 TSA Plus, Opal 620 TSA Plus, and Opal 570 TSA Plus, respectively (all from AKOYA Biosciences, Marlborough, USA). The nuclei were counterstained using Spectral DAPI (AKOYA Biosciences, Marlborough, USA). (Gagiannis *et al.*, 2023)

2.6.3 Macrophage Phenotyping

Twelve lung tissue regions of interest were scanned to multispectral images (MSI) per sample using the 40x. magnification objective, corresponding to a tissue area of 334x250 μm^2 each. Scanning was performed using the VECTRA automated quantitative pathology imaging system (Perkin Elmer, Waltham, USA). After deploying automated cell detection using the InForm Software (Perkin Elmer, Waltham, USA), an in-built cell phenotyping algorithm was trained to detect CD16+, CD16/CD163+, CD68+, and CD68+/CD163+ cells, as well as a final cell type containing all other cells. S100A9-Expression was automatically assessed in the detected and classified cells in four bins (0-3) and calculated an H-Score of S100A9-Expression. After training, the final algorithm analyzed all samples in one batch. Measurement outputs of the InForm Software were analyzed in R version 4.0.3 using the phenoptr (v0.3.2) and phenoptrReports (v0.3.3) packages. (Gagiannis *et al.*, 2023)

2.6.4 Electron Microscopy

Lung tissue was immersion-fixed with 4% paraformaldehyde in 0.1M PBS with a pH of 7.4. After several washing procedures in 0.1M PBS, the tissue was osmicated with 1% OsO4 in 0.1 M cacodylate and dehydrated in increasing ethanol concentrations epon infiltration, and flat embedding was performed following standard procedures. Methylene blue was used to stain semithin sections of 0.5 µm. Seventy to ninety-nanometer-thick sections were cut with an Ultracut UCT ultramicrotome (Fa. Reichert, Wetzlar, Germany) and stained with 1% aqueous uranylic acetate and lead citrate. The samples were then examined with a Zeiss EM 109 electron microscope (Fa. Zeiss, Jena, Germany), which was coupled to a TRS USB (2048x2048, v.596.0/466.0) camera system with ImageSP ver.1.2.6.11 (x64) software. (Gagiannis *et al.*, 2023)

3.0.0 Results

3.1.0 General Cohort Characteristics

This cohort consisted of a young group of subjects with a median age of 40, ranging from 18 to 80.
29 of the 51 subjects were male; the remaining 21 were women. None of the subjects suffered any pulmonary diseases, which could falsify the outcome of the data.
There was no case of hospitalization throughout the exclusively mild-moderate progressions of COVID-19. All subjects were unvaccinated throughout the entire period of the study. The median period post-infection was 17 weeks. (Gagiannis *et al.*, 2023)

3.2.0 Diagnostic Scheme

The patients in the cohort were examined between November 2020 and March 2021 at the Bundeswehrkrankenhaus (army hospital) in Ulm, Germany. All subjects consented to the proposed diagnostic examination methods, such as radiological imaging, serology, and bronchoscopy. The patients also approved the publication of the collected data and the use of the biopsies for this research. This study was conducted per the guidelines of the Declaration of Helsinki. The ethics committee in Ulm had previously endorsed it under reference number 129-20 and 331/20.
Sixty-six patients suspected of having PASC-ILD underwent a comprehensive physical examination, medical history assessment, and spiroergometry. An ANA/ANCA/ENA screening was conducted as described in the previous section. After ruling out other causes for dyspnea or respiratory impairment, fifty-one patients were identified as the final cohort. To evaluate for potential PASC-ILD, these fifty-one subjects underwent high-resolution computed tomography (HR-CT), biopsies (n=51), and/or bronchoalveolar lavage (n=18) for immunoassays. For comparison, autopsy samples (n=15) were included from individuals who had died of non-pulmonary causes. The diagnostic scheme is illustrated in **Figure 6** below. (Gagiannis *et al.*, 2023)

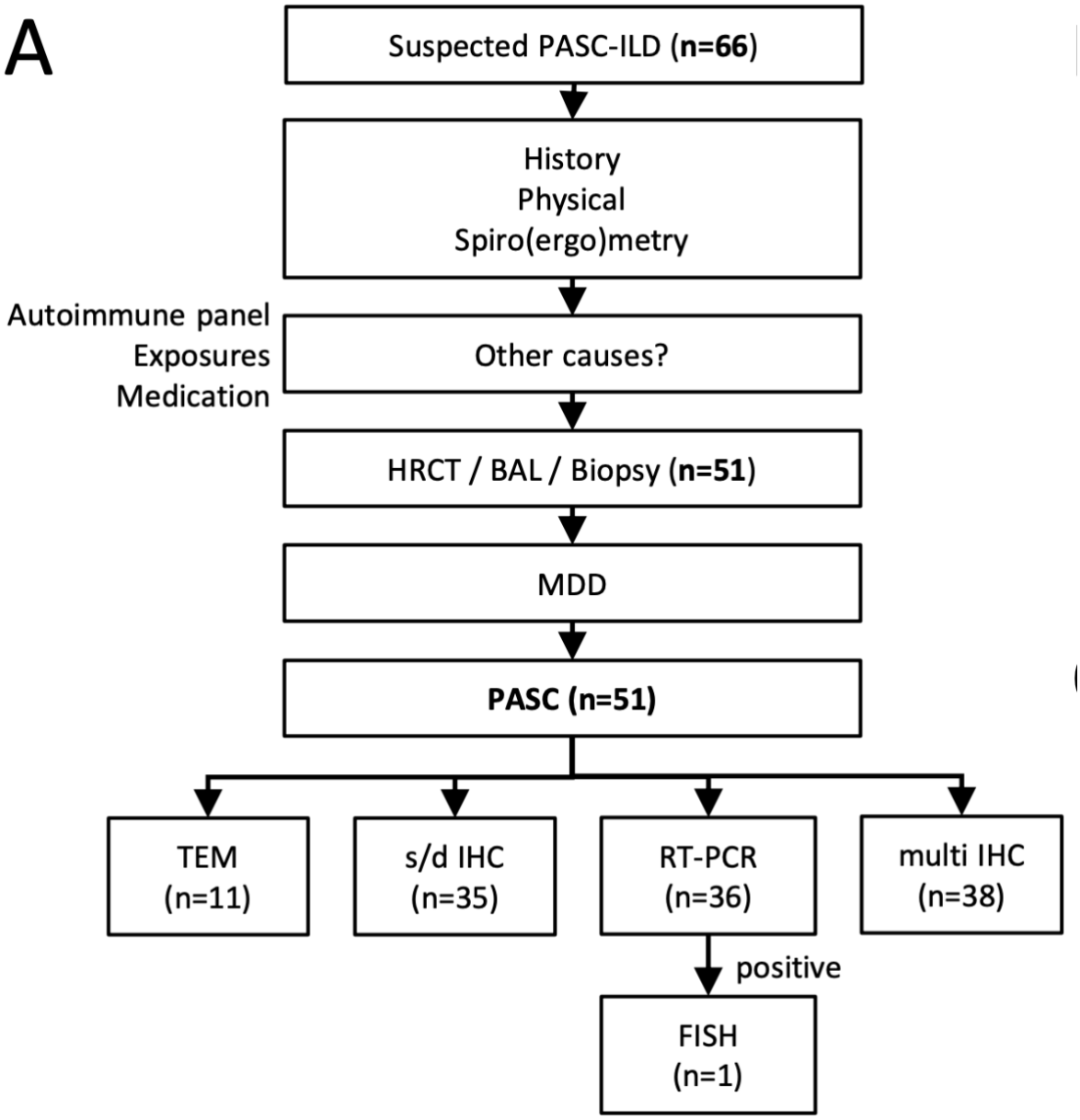

Figure 6 Workflow of the diagnostic scheme used to select the PASC patient cohort, University Hospital Ulm, 2020-2022 (Gagiannis et al., 2023). *66 PASC-ILD patients were admitted to the study. These underwent physical examinations, spiroergometry and a medical history evaluation. 51 out of these 61 patients were then admitted to HRCT/BAL/Biopsies. 11 were subsequently moved on to Transmission Electron Microscopy (TEM), 35 into immunohistochemistry (IHC), 36 into Reverse Transcription Polymerase Chain Reaction (RT-PCR), 38 into multi-immunohistochemistry (IHC), and one into fluorescence in situ hybridization (FISH). Post-acute Sequelae of COVID-19 (PASC), Post-acute Sequelae of SARS-CoV-2 interstitial lung disease (PASC-ILD), High resolution computer tomography (HRCT), Bronchoalveolar lavage (BAL)*

3.3.0 Clinical Results

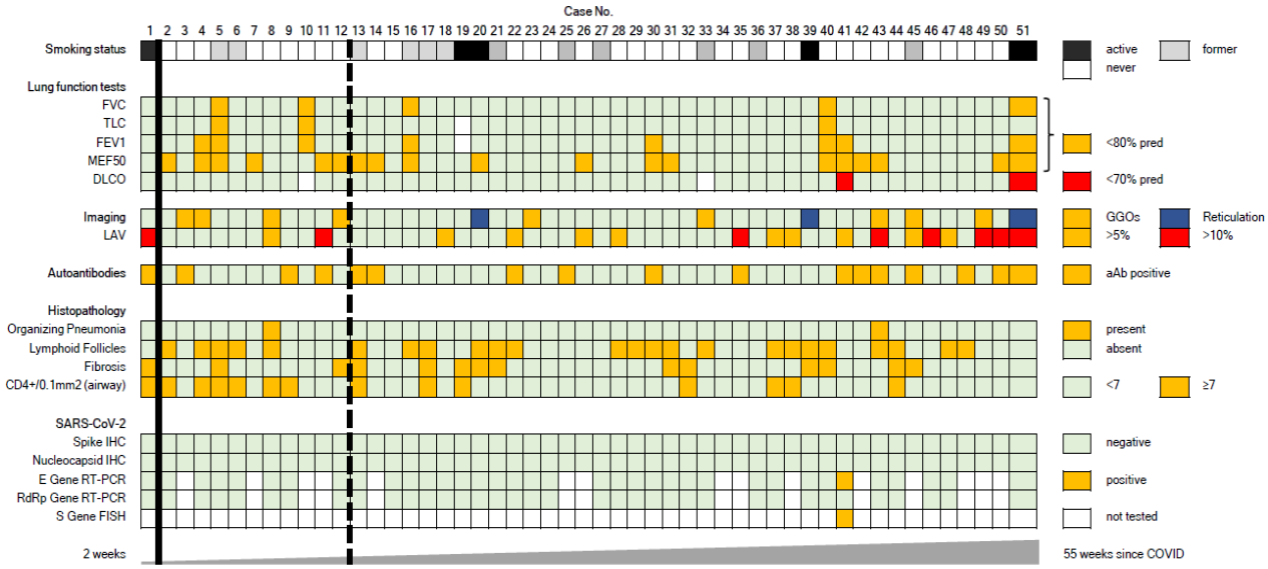

***Figure 7 Clinical, histopathological, serological, and radiological results of 51 PASC subjects between 2 and 55 weeks since COVID, University Hospital Ulm, 2020-22 .*(Gagiannis *et al.*, 2023)** *These have been chronologically listed in this heat map. The first line signifies four weeks, the second dotted line indicates week 12. 9.8% (5 subjects) and 23.5% (12 subjects) of the 51 were smokers of past smokers. Autoantibodies (antinuclear antibody titer ⩾1:320 and/or positive immunoblot for Scl-70, proliferating cell nuclear antigen, PM-Scl, double-stranded DNA, SS-B, histone, or rheumatoid factor >20 U/ml) were detected in 17 (33.3%) of 51 patients. Median FVC, TLC, FEV1, maximal expiratory flow at 50% of FVC (MEF50), and DLCO (percent predicted) were 94 (interquartile range, 87–102), 102.5 (93–111), 95.5 (85–102), 91 (69–104), and 94 (87–113), respectively. Median FEV1/FVC was 1 (0.95–1.04) and LAV was >5% in 18 (35.3%) of 51 patients. (*Gagiannis *et al.*, 2023*) FISH analysis was performed only in the single patient with positive SARS-CoV-2 RT-PCR (case 41). autoantibodies (aAb) fluorescence in situ hybridization (FISH); ground-glass opacities (GGOs); immunohistochemistry (ICH); Reverse transcription polymerase chain reaction (RT-PCR), Forced vital capacity (FVC), Total lung capacity (TLC), forced expiratory volume in one second (FEV1), diffusing capacity of the lung for carbon monoxide, bronchoalveolar lavage (BAL), Interquartile range (IQR), maximal Expiratory Flow at 50% of Forced Vital Capacity (MEF50), Lung attenuation value (LAV), diffusing capacity of the lung for carbon monoxide (DLCO), Post-acute Sequelae of (COVID-19) (PASC)*

The most striking spiroergometric findings revealed that 15.7% and 37.7% of the subjects had an FEV1 and FVC value below 80%, respectively. Additionally, a significantly altered MEF 50 value below 80% was observed, in 17 cases in the tissue cohort and 10 in the BAL cohort. The median oxygen pulse (VO2/HF) stood at 13.5, falling within an interquartile range of 10-15. When considering the total lung capacity (TLC), only 5.88% (3 out of 51 patients) had a value less than 80% pred. reduced DLCO below 70% was detected in 3.9% of convalescents, ranking as one of the most frequently identified pathological parameters. The numerical values are displayed in **Table 7.** (Gagiannis *et al.*, 2023)

Table 7 Baseline clinical characteristics and assessment of lung function in PASC Patients, University Hospital Ulm, 2020-2022. (*Gagiannis *et al.*, 2023*) *PASC. We can see an increase in the FVC, FEV1, and a decrease in the VO2/HF. Forced vital capacity (FVC), total lung capacity (TLC), forced expiratory volume in one second (FEV1), diffusing capacity of the lung for carbon monoxide (DLCO), bronchoalveolar lavage (BAL), interquartile range (IQR), maximal expiratory flow at 50% of forced vital capacity (MEF50), lung attenuation value (LAV), post-acute sequelae of COVID-19 (PASC)*

Characteristics	PASC patients (tissue cohort) (n=51)	PASC patients (BAL cohort) (n=18)	p-value
Age (years; median, range)	40.0 (18-80)	46.0 (20-82)	0.4742
Gender (%) **Female** **Male**	 22.0 (43) 29.0 (57)	 7.0 (39) 11.0 (61)	 0.7889
Weeks since SARS-CoV-2 (median, range)	17.0 (2-55)	22.0 (12-108)	**0.0052**
Presence of autoantibodies* (n, %)	17.0 (33.3)	7.0 (38.9)	0.7754
FVC, % pred (median IQR)	94.0 (87-102)	90.0 (37-110)	**0.0201**
TLC, % pred (median, IQR)	102.5 (93-111)	97.0 (54-149)	0.4343
FEV1, % pred (median, IQR)	95.5 (85-102)	89.5 (44-105)	**0.0229**
DLCO, % pred (median, IQR)	94.0 (87-113)	87.0 (43-132)	0.0798
VO2/HF (median, IQR) (n=29)	13.5 (10-15)	10.5 (7.2-19)	0.2776
Low FVC <80% pred, n (%)	5.0 (9.8)	4.0 (22.2)	0.2259
Low TLC <80% pred, n (%)	3.0 (5.9)	3.0 (16.7)	0.1781
Low FEV1 <80% pred, n (%)	8.0 (15.7)	3.0 (16.7)	>0.9999
Low DLCO <70% pred, n (%)	2.0 (3.9)	3.0 (16.7)	0.1072
LAV >5%, n (%)	18.0 (35.3)	n.a.	n.a.
MEF 50	17.0 (42.9)	10.0 (55.5)	0.3967
BAL Lymphocyte count (median, IQR) CD4/CD8 ratio (median, IQR)	 13.0 (8-20) 2.2 (1.6-3.2)	 12.0 (7-27) 3.2 (0.95-5.8)	 0.6312 0.2782
* ANA titer ≥ 1:320 and/or positive IB (Scl-70, PCNA, PM-Scl, dsDNA, SS-B, Histone or RF >20U/ml			

The RV and VO2/HF improved over time since infection **Figure 8.** Between twenty- and sixty weeks post-infection, parameters seem to return to normal. The correlation of VO2/HF with weeks since the COVID-19 infection achieved statistical significance, with a p-value of **0.00879** (<0.01). (Gagiannis *et al.*, 2023)

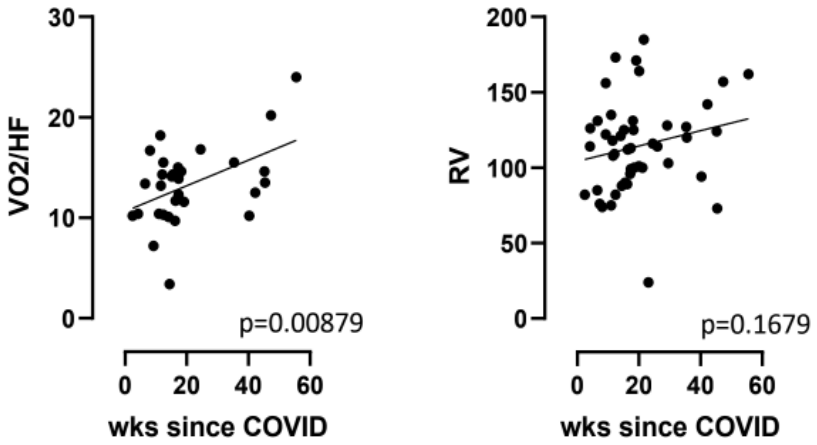

Figure 8 Improvement of VO2/HF and RV over weeks (0-60 weeks) in patients since COVID-19 infection, University Hospital Ulm, 2020-2022 (*Gagiannis *et al., 2023)*.* Coronavirus Disease 2019 (COVID-19), Residual volume (RV), oxygen consumption over heart rate (VO2/HF), weeks (wks)

3.4.0 Imaging Results

The imaging data identified reticulations in the HRCT for 3 out of 51 patients, constituting 5.9%. Additionally, 9 out of 51 subjects (17.6%) exhibited ground-glass opacities (GGO), as displayed in **Figure 9.**

35.3% of the patients had a low attenuation volume (LAV being less than -950 Hounsfield units) of more than 5% on the HRCT. Within this group, 15.7% showed areas with an LAV exceeding 10%. (Gagiannis *et al.*, 2023)

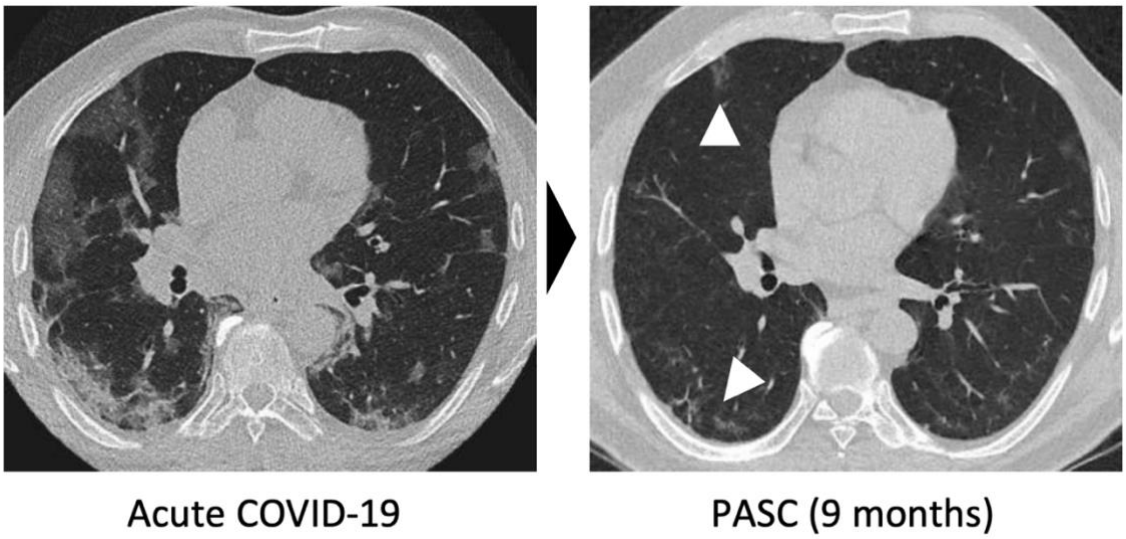

***Figure 9 Radiological results showing the ground-glass opacities (arrowheads) and reticulations in PASC patients (right), in contrast to Acute COVID-19 patients (left), University Hospital Ulm, 2020-2022.* (Gagiannis et al., 2023)** *Post-acute Sequelae of SARS-CoV-2 (PASC), Coronavirus Disease 2019 (COVID-19)*

3.5.0 Serological results

The results consist of the tested parameters for 51 biopsy and 18 BAL PASC patients. Autoantibodies were detected in 17 of the 51 patients (33.3%). In the immunoblot, these tested positive for Scl-70, PCNA, PM-Scl, dsDNA, SS-B Histones, or exhibited a raised ANA titer of 1:320 or higher. In the bronchoalveolar lavage (BAL) fluid, the median lymphocyte count was 13. The interquartile range (IQR) spanned from 8 to 20. Furthermore, the ratio of CD4 to CD8 lymphocytes in BAL fluid was 2.2. The variability of this ratio, represented by its IQR, ranged between 1.6 and 3.2. (Gagiannis *et al.*, 2023)

3.6.0 Histopathological Findings and Tissue-based SARS-CoV-2 Detection

Table 8 presents an overview of the histopathological findings of 51 transbronchial biopsies from PASC patients compared to 15 control tissue samples. 4% of convalescents exhibited signs of organizing pneumonia. None of the tissue samples from the autopsy controls displayed any evidence of organizing pneumonia. While 40% of the controls did not exhibit centrilobular lymphoid follicles, 47% of the PASC cohort did, with a p-value of 0.5580. (Gagiannis *et al.*, 2023)

Table 8 Lung histology and spatial T lymphocyte subtyping in 51 post-COVID patients and pre-pandemic autopsy controls, University Hospital Ulm, 2020-2021. (Gagiannis et al., 2023) *Post-acute Sequelae of SARS-CoV-2 (PASC), Cluster of Differentiation 4 positive (CD4+), Cluster of Differentiation 8 positive (CD8+), Interquartile Range (IQR), Transmission electron microscopy (TEM)*

Characteristics	PASC (n=51)	Autopsy controls (n=15)	p-value
Age (years; median, range)	40 (18-80)	56 (25-82)	0.0006
Gender			
Female	22 (43%)	5 (33%)	0.5627
Male	29 (57%)	10 (67%)	
Organizing Pneumonia			
Present	2 (4%)	0	>0.999
Absent	49 (96%)	15 (100%)	
Lymphoid follicles			
Present	24 (47%)	6 (40%)	0.5580
Absent	27 (53%)	9 (60%)	
Interstitial fibrosis			
Light microscopy, n (%)	14/51 (27%)	2 (13%)	0.3262
TEM, n (%)	11/11 (100%)	n.a.	
Small airways (n=35) (bronchi/bronchioles)			
CD4+ cells/0.1mm² (IQR)	6.7 (4-8)	3.7 (3-5)	0.0154
CD8+ cells/0.1mm² (IQR)	4.2 (1-6)	2.4 (1-4)	0.1327
CD4/CD8 ratio (IQR)	2.6 (1.2-12)	2 (1-5)	0.8487
Interstitium (alveolar septae) (n=35)			
CD4+ cells/0.1mm² (IQR)	4.6 (3-5.5)	2.2 (1-3)	0.067
CD8+ cells/0.1mm² (IQR)	2.8 (1-4)	2.2 (1-3)	0.8794
CD4/CD8 ratio (IQR)	2.4 (1.3-8)	1.3 (1-2)	0.2626

Using the Masson-Goldner staining and upon examining the tissue samples, interstitial fibrosis was observed in 14 out of 51 samples (27%) as shown in **Figure 10.**

Only 7 out of 51 (13%) of the controls displayed signs of fibrosis (p=0.3262). We conducted an ultrastructural analysis on a subset of 11 from the aforementioned 14 fibrosis samples. All 11 (100%) exhibited interstitial deposition of collagen. Centrilobular lymphoid follicles were identified in 24 out of 51 cases (47%). In contrast, only 6 out of the 15 controls (40%) presented evidence of these structures (p=0.5580). Given that residual SARS-CoV-2 or its viral fragments in the tissue might be

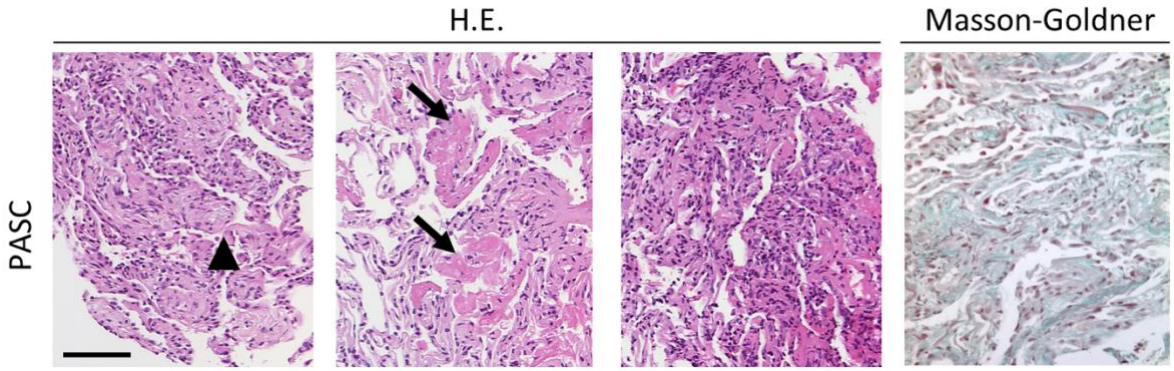

Figure 10 Lung tissue biopsies of PASC patients in H.E. and Masson-Goldner staining, University Hospital Ulm, 2020-2021. (*Gagiannis *et al., 2023) *In the H.E. stained biopsy tissues shown on the left, arrows indicate organizing pneumonia (triangle tip) and alveolar fibrinous exudate (straight arrows). The image on the right illustrates interstitial lymphocytosis. The Masson-Goldner stained image clearly demonstrates minimal interstitial fibrosis. The scale bar represents 100µm. Post-acute Sequelae of SARS-CoV-2 (PASC), Hematoxylin and Eosin staining (H.E.)*

responsible for chronic inflammation, immunohistochemistry for N and S proteins was utilized. The conventional RT-PCR test was used to test for the RdRp gene. All tests concluded with negative results, indicating no residual viral structures. However, during the RT-PCR testing, patient case no. 41 tested positive for an E gene found in the alveolar epithelium. A SARS-CoV-2 FISH analysis was performed to validate this finding, which also tested positive **Figure 11.** (Gagiannis *et al.*, 2023)

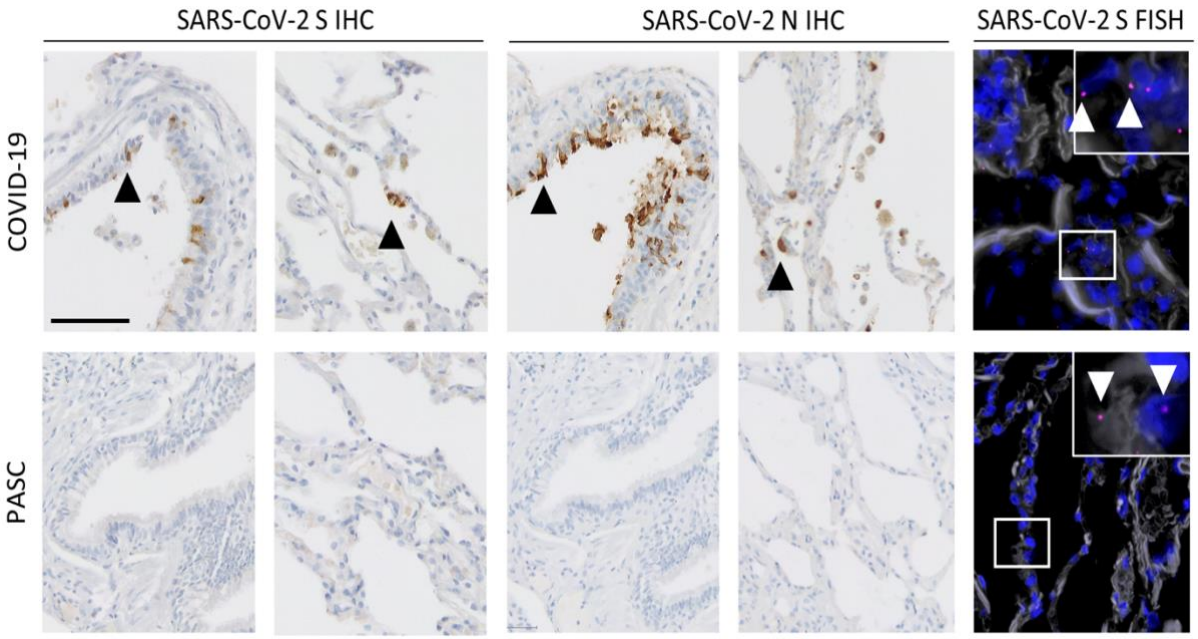

Figure 11 Immunohistochemistry of lung tissue in PASC and COVID-19 biopsies, University Hospital Ulm, 2020-2021. (*Gagiannis *et al.*, 2023*) *N,S proteins and the RT-PCR for the RdRp gene were negative in the immunohistochemistry. One subject tested positive in the RT-PCR for the E-gene which was later confirmed in the FISH-analysis. Post-acute Sequelae of SARS-CoV-2 (PASC), immunohistochemistry (IHC), Fluorescence In Situ Hybridization (FISH), Coronavirus Disease 2019 (COVID-19), Severe Acute Respiratory Syndrome Coronavirus 2(SARS-CoV-2).*

To summarize the histopathological findings and the results of tissue-based SARS-CoV-2 detection, organizing pneumonia, fibrinous alveolitis, and increased interstitial lymphocytosis in the bronchi and bronchioles could be observed.

3.7.0 Spatial T-lymphocyte Subtyping in PASC Patients and Autopsy Controls.

The quantifiable results are presented in **Table 8.** When examining the interstitial tissue and tissue around small airways, it was observed that most CD3+ T-cells were CD4+ cells. 35 tissue samples were tested from both areas. Around the small airways, 6.7 CD4+ cells/0.1mm² (p=0.0154) and 4.2 CD8+ cells/0.1mm² (p=0.1327) were identified. The CD4/CD8 ratio is 2.6. The CD4/CD8 ratio in the interstitium is 2.4, without a significant difference. 4.6 CD4+ cells/0.1mm² and 2.8 CD8+ cells/0.1mm² could be found within the septa. **Figure 12** (Gagiannis *et al.*, 2023)

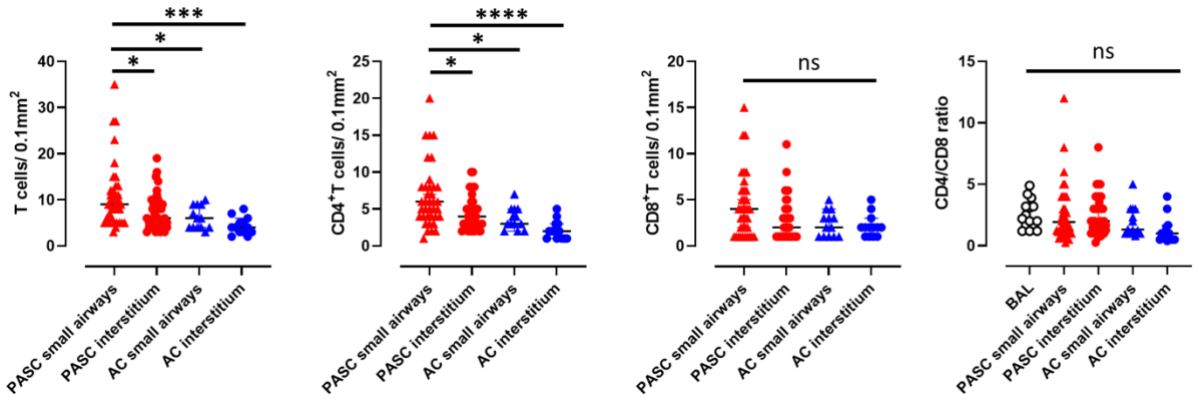

Figure 12 Comparison of the T cell, CD4+ T-cell, CD8+ T-cell and CD4/CD8 ratio in PASC patients and autopsy controls in the small airways in interstitium, University Hospital Ulm, 2020-2021. (*Gagiannis *et al.*, 2023*) *All parameters are elevated in PASC patients, in both the small airways and interstitium. The concentration of CD3+ and CD4+ T-helper cells in the small airways is notably higher compared, to the interstitium in PASC patients and both airways and the interstitium in autopsy controls (*Gagiannis *et al.*, 2023*). Cluster of Differentiation 4 positive (CD4+), Cluster of Differentiation 8 positive (CD8+), Post-acute Sequelae of SARS-CoV-2 (PASC), Air condition (AC), Bronchoalveolar lavage (BAL)*

As shown in **Figure 12**, the total concentration of T-cells/0.1mm² was significantly higher in the small airways of PASC convalescents. The number of T-lymphocytes in the septa was lower, but compared to control groups, the levels were still notably higher. As noted, the most significant observation is the high concentration of CD4+ cells in the small airways of convalescents. This parameter achieved statistical significance with a p-value of 0.0 (6.7 CD4+ cells/0.1mm²). CD8+ T-cells were also higher in the bronchi/bronchioles compared to the interstitium, but this could not reach statistical significance. (Gagiannis *et al.*, 2023)

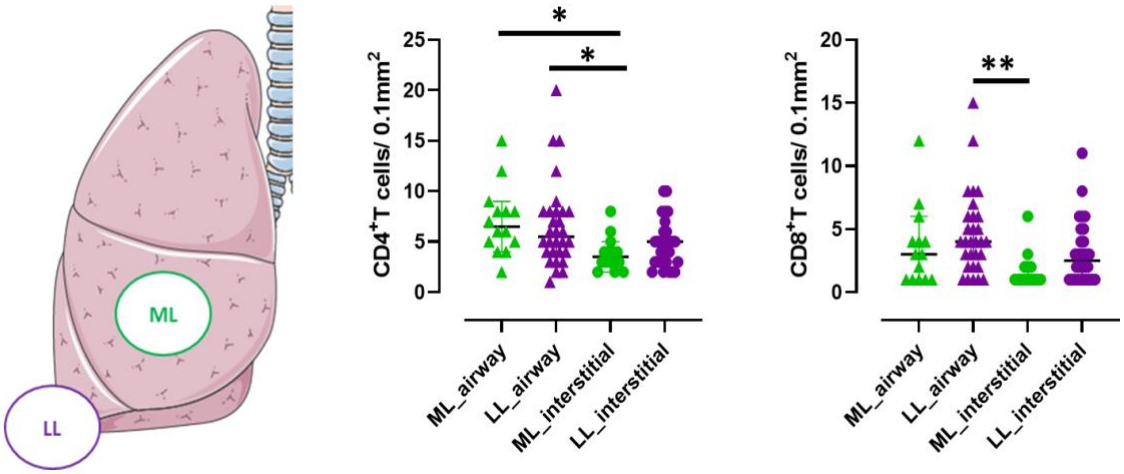

Figure 13 Spatial distribution of CD4+ and CD8+ T cells within the lower and middle lobe of the lung, University Hospital Ulm, 2020-2021. (Gagiannis et al., 2023) *Middle lobe (ML), Lower lobe (LL), Cluster of Differentiation 4,8 positive (CD4/8+), Post-acute Sequelae of*

Figure 13 depicts the distribution of T-cells in the middle and lower lobes of the lung, as well as in the airways and interstitial fluid. The inflammatory T-cell fluid is primarily situated in the small airways rather than the lung septa. **Figure 14** also confirms that CD3+ and CD4+ t-cells concentration is notably higher in the small airways than in the interstitium. (Gagiannis *et al.*, 2023)

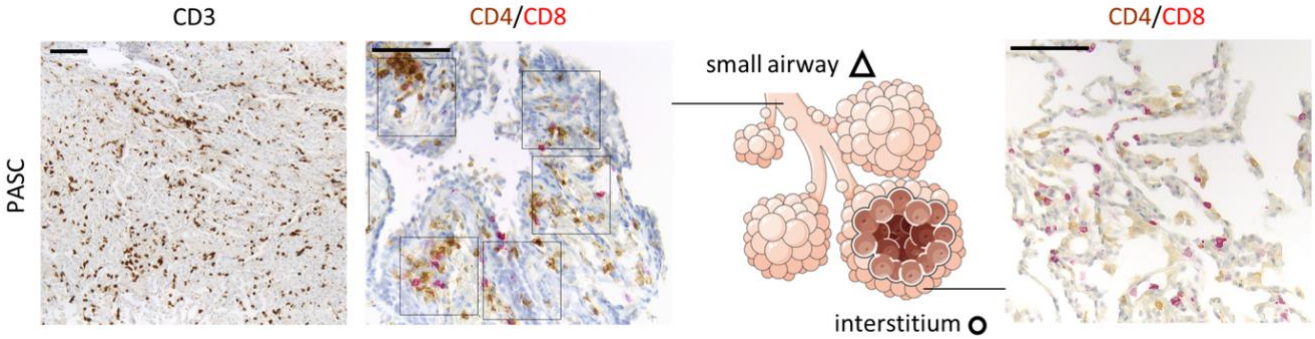

Figure 14 Microphotographs of immunochemically double-stained cells in PASC biopsies of the small airways and interstitium, University Hospital Ulm, 2020-2021. (Gagiannis et al., 2023) *On the left are CD3-cells, followed by CD4/CD8 around the bronchioli, and CD4/CD8 in the interstitium on the right. The scale bar represents 100µm. Cluster of Differentiation 3,4,8 positive (CD3/4/8+), Post-acute Sequelae of SARS-CoV-2 (PASC),*

3.8.0 Assessment of Interstitial Fibrosis and Quantification of Macrophage Subpopulations in PASC Patients.

Of the 14 PASC samples that tested positive for fibrosis during light microscopy, ultrastructural analysis (TEM) was conducted on a subgroup of 11 from those 14 samples. In all 11 subjects, established collagen fibrils could be identified, as depicted in **Figure 15**. (Gagiannis *et al.*, 2023)

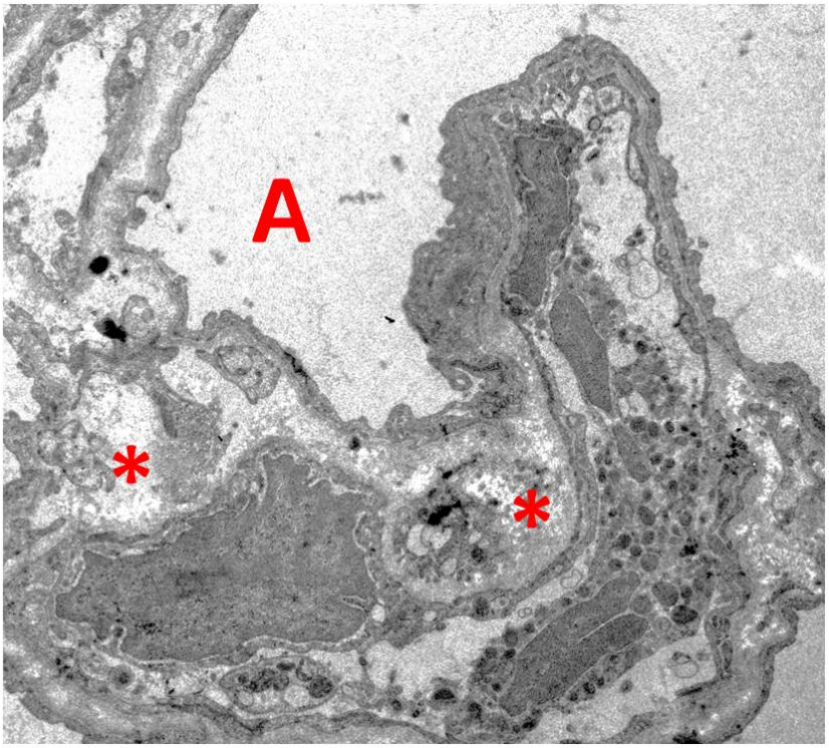

Figure 15 Microphotograph transmission electron microscopy of lung tissue in PASC patients to demonstrate collagen fibrils (*) in 11 of 14 patients, University Hospital Ulm,2021-2022. (Gagiannis et al., 2023) *Alveolus (A)*

Figure 16 also presents the results of the immunofluorescence multiplex staining used to identify macrophage subpopulations. Additionally, an investigation of macrophage phenotypes associated with fibrotic processes (CD16/CD68/CD163/S100A9) was conducted. (Gagiannis *et al.*, 2023)

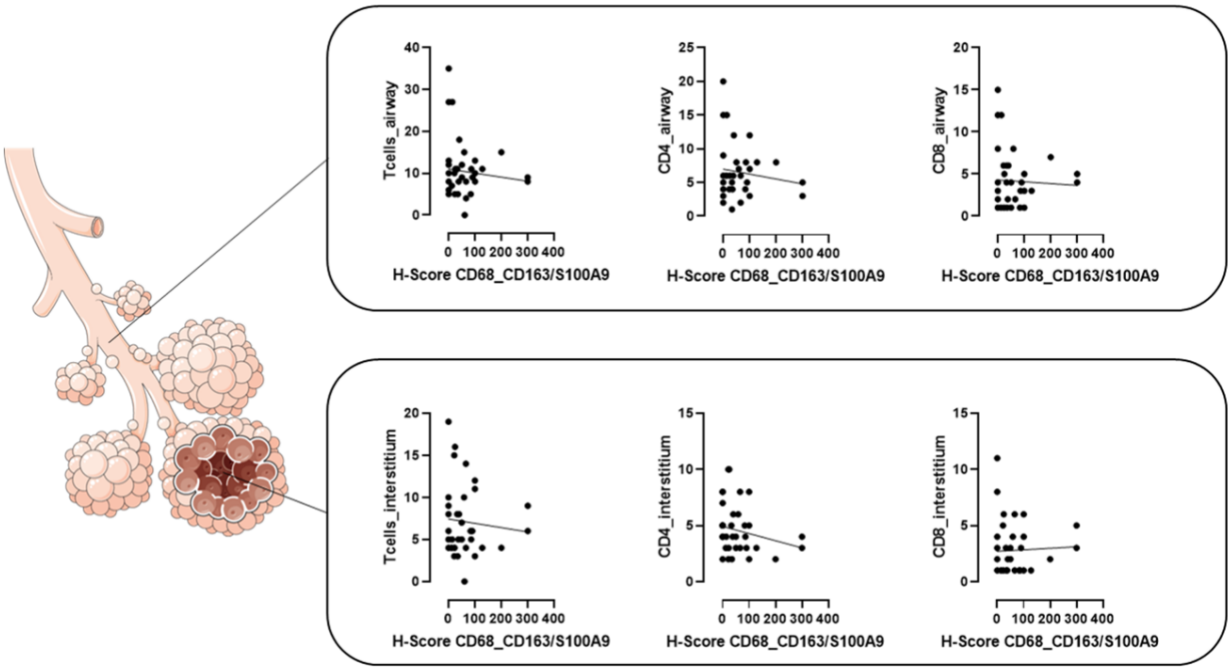

Figure 16 H-Scores for the pro-fibrotic macrophages (CD68/CD163/S100A9) and CD4+/CD8+ around the airways and alveolar septa in PASC biopsies, University Hospital Ulm, 2020-2021. (Gagiannis et al., 2023) *Cluster of Differentiation 4/8 positive (CD4+/CD8+),*

The quantifiable results are seen in **Table 9.**

***Table 9 Macrophage panel staining and automated quantitative imaging. H-scores (CD16/CD68/CD163/S100A9) and CD cell concentrations in 38 PASC patients, University Hospital Ulm, 2020-2021*. (Gagiannis *et al.*, 2023)** *Post-acute sequelae of COVID-19 (PASC), Cluster of Differentiation (CD)*

Characteristics	**PASC (n=38)**
Age (years; median, range)	39.5 (18-82)
Gender	
Female	23 (44%)
Male	29 (56%)
Cells/mm² (median, IQR)	
CD68+	26 (14-46)
CD16+	116 (17-539)
CD16+/CD163+	151 (72-258)
CD68+/CD163+	6 (1-77)
H-scores	6 (2-22)
S100A9+ (other cells)	2 (0-9)
CD68+/S100A9+	39 (13-61)
CD16+/S100A9+	221 (123-252)
CD68+/CD163+/S100A9+	34 (0-85)

Figure 17 indicates no distinct trend correlating the presence of pro-fibrotic macrophages with factors such as gender, location (middle or lower lobe), and lymphocyte distribution in BAL, DLCO, or Co2/HF.

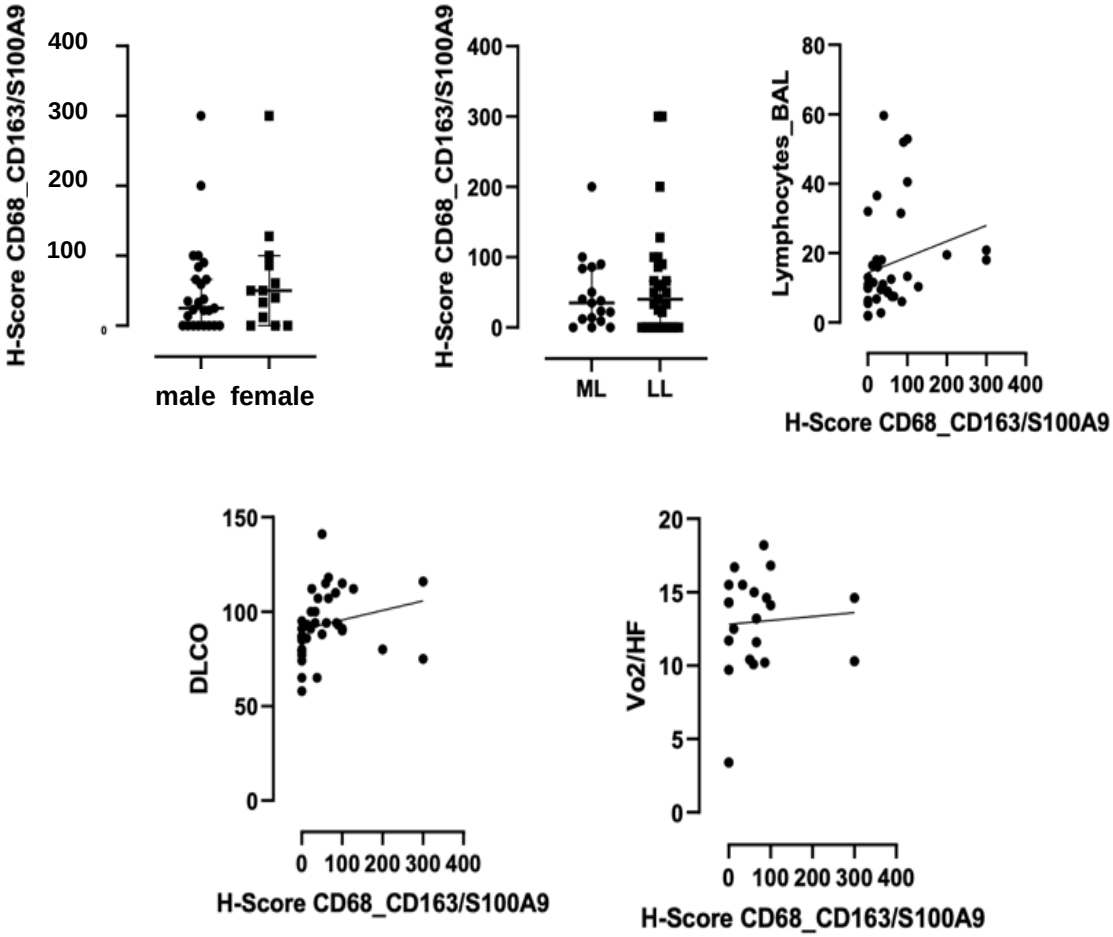

Figure 17 Levels of H-scores of pro-fibrotic macrophages CD68/CD163/S100A9 and CD4+/CD8+ in the small airways and interstitium of PASC patients, University Hospital Ulm, 2020-2021. (Gagiannis et al., 2023) *Middle lobe (ML), Lower lobe (LL), bronchoalveolar lavage (BAL), Diffusing Capacity of the Lung for Carbon Monoxide (DLCO), oxygen consumption over heart rate (VO2/HF)*

Figure 18 displays the results of the conducted Legendplex immunoassay, which was used to analyze various cytokine phenotype levels (IL-1β, IL-6, TNF-α, IFN-λ1, IL-8) in the BAL fluid of PASC patients and a control group. Most cytokine types exhibited similar concentration levels in the PASC and controls cohorts. However, an elevated concentration of IL-1β was observed in PASC patients compared to the control group, reaching statistical significance with a p-value of **0.012** ($p<0.05$). While IL-8 cytokines were also more prevalent compared to the controls, they did not achieve statistical significance, with a p-value of 0.155. (Gagiannis *et al.*, 2023)

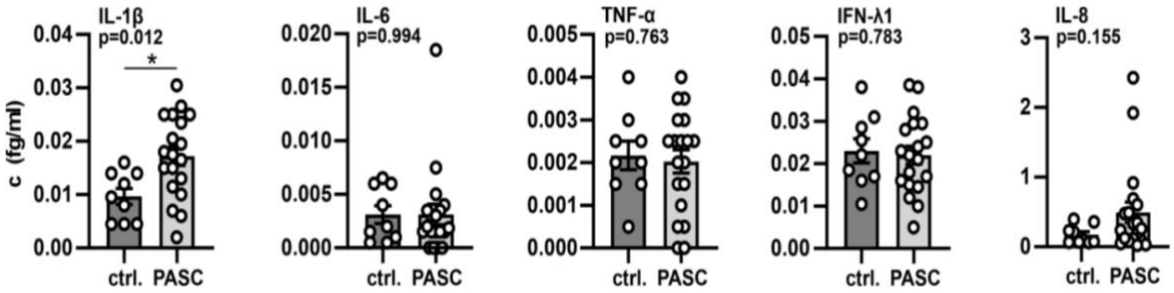

Figure 18 Interleukin levels in BAL Fluid of PASC and control patients were tested using legendary immunoplex essays, University Hospital Ulm, 2020-2021. **(Gagiannis et al., 2023)** *The levels of IL-8, TNF-α, IL-6, IL-1β, and IFN-λ1 were determined. IL1-β and IL-8 were increased in comparison to controls. However, the parameter could not reach statistical significance. Interleukin (IL), Tumor necrosis factor-alpha (TNF-α), interferon delta 1 (IFN-γ1), post-acute sequelae of COVID-19 (PASC), control (ctrl.)*

4.0.0 Discussion

Many COVID-19 convalescents experience long-term symptomatic patterns, as highlighted in the introduction. This phenomenon is referred to as post-acute sequelae of COVID-19 (PASC). This piece aims to delineate the characteristics of these symptomatic patterns by utilizing radiological, clinical, histopathological, and serological parameters to refine the understanding of PASC's broad spectrum. In light of the results, it was important to explore the relationship between PASC and elevated levels of cytokines and autoantibodies to determine if they contribute to a persistent inflammatory process in the lung. Additionally, it was examined whether residual viral fragments in the tissue could be the primary cause of PASC (Merad *et al.*, 2022). Traits of other bronchial abnormalities was compared with the data to identify parallels. (Gagiannis *et al.*, 2023)

51 subjects were enrolled in the study at the Bundeswehrkrankenhaus (army hospital) in Ulm, Germany, between November 2020 and March 2021. After obtaining written consent from each patient, a rigorous diagnostic scheme was implemented to gather radiological, clinical, histopathological, and serological data. Distinct from other PASC studies, there was an advantage of examining the early phase of the pandemic before COVID-19 vaccinations became widely available. As a result, it was possible to evaluate the unaltered impact of COVID-19 on the human body. Another unique characteristic of the cohort is the younger age of the patients, primarily because the majority are soldiers from the army hospital. This also explains why most were male (57%). None of the subjects had co-morbidities that might have falsified the data results. (Gagiannis *et al.*, 2023)

Most of the patients reported symptoms of dyspnea and fatigue. Spiroergometric results did not indicate a significant decline in lung function within the group. However, a key finding was the presentation of an obstructive pattern in the subjects, as evidenced by a reduced FEV1, FVC, and an increased LAV. Moreover, the MEF50 was notably diminished in both the tissue and the BAL cohort. Compared to the control group, a significantly increased concentration of CD4+ cells in the small airways was observed**.** The elevated levels of IL-1β cytokines were also statistically significant. Histopathological findings revealed more instances of

organizing pneumonia and fibrinous deposits. Residual viral material was detected in only one patient and did not significantly contribute to the observed pathological processes. However, evidence of fibrotic remodeling and pro-fibrotic macrophages was established. (Gagiannis *et al.*, 2023)

4.1.0 Data Analysis: The Link of PASC to Elevated Autoantibodies and T-cells

The elevated concentration of CD4+ lymphocytes in bronchioles (p=0.0154) couldn't be associated with specific symptoms or clinical or radiological patterns. However, there is an inverse correlation between the increase VO2/HF over time post-infection. The number of T-cells in small airways also declines over the weeks. As a result, the decreasing concentration of CD4+ cells might indicate recovery of lung function and slowing inflammatory processes. Yet, of all the mentioned trends, only the correlation between VO2/HF over time reached statistical significance with a p-value of **0.00879**. (Gagiannis *et al.*, 2023)

This finding challenges the assertion that CD8+ T-cells and their destructive characteristics are responsible for tissue degeneration. (Cheon *et al.*, 2021)

Evidence suggests that, in milder cases of COVID-19, T-cells activate cytokines. In more severe cases, there's a shift toward producing CD8+ cells, leading to cytotoxic predominance. Since most of this cohort experienced a mild-to-severe progression, it might explain why most of the infiltrate was composed of CD4+ T-cells, resulting in lesser tissue destruction. Moreover, studies indicate that these milder, CD4+ dominant cases only demonstrate a notable T-cell concentration for 3-5 months before it diminishes. (Littlefield *et al.*, 2022)

4.2.0 The Link Between Persisting Viral Components and Chronic Inflammation

The second hypothesis stemmed from evidence suggesting that lingering Sars-CoV-2 viral fragments might be associated with a continuous immune response, resulting in a chronic inflammatory process. Of the 51 RT-PCR tests conducted, all were negative except for the test from patient case number 41, which showed a positive result for the E gene **Figure 6.** This presence of viral mRNA was subsequently confirmed by FISH 35 weeks post-infection. The residual viral

components were identified in the epithelial wall of the lung. Nevertheless, it was not possible to associate this finding with any pathological symptoms induced by PASC. (Gagiannis *et al.*, 2023) This implies that the destructive processes, which result in tissue damage and diminished lung function, likely initiate after the virus is cleared from the body.

Support for this assertion can also be found in a study of COVID-19 convalescents. Transbronchial biopsies (TBB) were taken at various stages of infection progression and from additional tissue samples later. Diffuse alveolar damage (DAD) was diagnosed in patients testing positive for COVID-19. As the viral load decreased, signs of fibrosis became evident. This fibrosis continued to progress even after the virus was cleared from the system. (Gagiannis *et al.*, 2021) Thus, it can be infered that the pathological processes resulting in lung tissue damage are probably not due to viral fragments remaining in the body but stem from a different cause.

4.3.0 Do Antibodies and Cytokines Play a Role in the Development of PASC, and If Yes, How?

A third (33.33%) of the cohort tested positive for Scl-70, PCNA, PM-Scl, dsDNA, SS-B, or Histones in the immunoblot or had an ANA titer of 1:320 or higher. Although many subjects displayed pronounced levels of autoantibodies, a clear correlation between elevated ANA/ENA titers and lung functionality tests, imaging, histopathological characteristics, GGO, or reticulations in imaging could not be established. However, a study indicates that heightened ANA/ENA concentrations are predominantly associated with more severe progressions of COVID-19 and arise from extrafollicular B-cell activation. This subsequently leads to excessive antibody production. (Gagiannis *et al.*, 2021; Gagiannis *et al.*, 2023)

Furthermore, the level of IL-β in BAL fluid in PASC patients was higher than controls to the extent that the data achieved statistical significance ($p=0.012$). IL-8 cytokines were also markedly elevated, but this variable did not attain statistical significance ($p=0.155$). (Gagiannis *et al.*, 2023) Evidence suggests that the cytokine storm triggered by superantigens triggers a surge of cytokines. This might be due to an ongoing infection or a hyperactive and unchecked immune response. In the case of an unregulated immune response, administering corticosteroids is recommended to inhibit such a response. (Jacobs, 2021) Since both the guidelines and the RECOVERY trial demonstrated that mortality rates decrease when prescribing

corticosteroids to COVID-19 patients with elevated cytokine levels, this could imply that the heightened interleukins are tied to an unrestrained immune response rather than an ongoing infection. (Jacobs, 2021; RECOVERY Collaborative Group *et al.*, 2021) The therapeutic efficacy of corticosteroids would also counter the theory of chronic inflammation resulting from enduring viral components.

4.4.0 What is the Cause of Pulmonary PASC?

Only a minority of the 51 patients in this cohort experienced significantly decreased lung function. Nevertheless, the most prevalent complication was a reduced FEV1 and FVC. The diminished forced expiratory volume, combined with a LAV of at least 5% in 35.5% of the cohort, is a common characteristic of obstructive lung dysfunction and small airway disease.

Evidence links the clinical and histological manifestations of IPAF (Interstitial Pneumonia with Autoimmune Features) to PASC. Since persistent viral matter does not cause post-COVID strains, IPAF/CTD-ILD must be considered as the cause. Many of its histological and radiological attributes, such as fibrotic deposition with collagen compartments, GGOs, reticulations, and increased T-cell levels, match the data. Additionally, there was evidence of fibrosis-associated macrophages and fibrotic tissue in a subgroup of this cohort.

However, other parameters, such as the distribution of CD4+ lymphocytes, were primarily observed in the small airways rather than in the interstitium. Furthermore, one criterion for IPAF is the presence of autoantibodies. Of the 51 patients, 17 presented with ANA/ENA titers of at least 1:320. However, to successfully confirm IPAF, surgical biopsies are mandatory, but they were not part of this study. Most importantly, since inflammatory signs were sparse in the interstitial space, this cohort does not qualify, and the hypothesis that IPAF is the cause of PASC can be dismissed. (Gagiannis *et al.*, 2023; Steinestel *et al.*, 2021)

Regarding the classification proposed by Ryu, there is a clear link between the serological, histological, and radiological findings and obliterative bronchiolitis. The obstruction of the airways leads to reduced MEF50, FEV1, FVC and an increase in LAV, resulting in a mosaic pattern in the HRCT. These components closely align with some of the most prominent features within this cohort. These three parameters essentially represent obstructed airflow within the bronchioles. Additionally, due to

chronic inflammation, elevated pro-fibrotic cytokine levels lead to fibrotic restructuring of lung tissue. (Ryu, Myers and Swensen, 2003) The 13% of patients who presented with fibrotic deposits and subjects with significantly elevated levels of IL-1β ($p=0.012$) also strongly support this hypothesis of present bronchiolitis. (Gagiannis *et al.*, 2023)

Interestingly, a study provided evidence that IL-1β is associated with fibrotic processes, as this specific cytokine subgroup was shown to induce spontaneous pulmonary fibrosis in mice. (Borthwick, Wynn and Fisher, 2013) Additionally, Ryu suggests that chronic obstructive pulmonary diseases such as obliterative bronchiolitis increase T-cell and macrophage distribution in the small airways. (Ryu, Myers and Swensen, 2003)

Considering that SARS-CoV-2 residual fragments were not detectable in almost every patient except for one, bronchiolitis following a mild COVID-19 indicates a generalized and non-specific response after the infection. Given that fibrotic structures could be identified in the cohort, along with the presence of pro-fibrotic macrophages and ILB-β interleukins in the BAL fluid, PASC patients must be consistently monitored. While the data shows that lung functionality in affected patients improves post-infection, monitoring is especially relevant since SARS-CoV-2 has been previously noted for its fibrotic processes.

4.5.0 Limitations

Fibrotic remodeling was examined, given its crucial role in the study. Pro-fibrotic macrophages and cytokines levels were assessed in lung tissue by conducting transbronchial biopsies (TBB). (Gagiannis *et al.*, 2023) However, it's recognized that fibrotic remodeling is focally distributed throughout the lung. TBB can often be an imprecise diagnostic tool, as focal fibrosis may not always be pinpointed during probing. For a definitive diagnosis of fibrotic NSIP patterns, a surgical biopsy would be necessary. (Ryu, Myers and Swensen, 2003) As such, it is inferred that the cohort's actual quantity of fibrotic tissue is likely more significant than what was identified.

Moreover, the diagnostic scheme didn't solely focus on mild-to-severe cases. The severity of disease progression can shape the pathological processes that are

observed. For instance, cases requiring hospitalization often display higher titers of ANA/ENA (Kamp *et al.*, 2023). The findings are restricted to the less severe cases.

Additionally, none of the participants had been vaccinated. Given recent advancements, most of the population has received at least one vaccine dose. Presently, the repercussions of contracting the virus are likely different.

Another limitation to consider is the composition of this cohort, which predominantly represents a specific gender and age group. As such, its findings are primarily representative of that demographic. Participants joined the study at various points post-infection. The sample sizes, ranging from 15 to 51, are relatively modest and may not achieve statistical significance.

Most notably, a more suitable control group would have comprised of transbronchial biopsies following viral infections other than SARS-CoV-2.

5.0.0 Summary

Numerous patients exhibit enduring symptoms following a Coronavirus Disease 2019 (COVID-19) infection, termed Post-Acute Sequelae of COVID-19 (PASC). The typical manifestations of PASC include fatigue, dyspnea on exertion, and cough. The speculated causes encompass the persistence of viral matter, chronic inflammation, or a dysregulated immune response aligning with radiologic abnormalities. The exact cause remains undetermined due to limited data availability. Hence, we have delineated an overview of the histological, radiological, and serological characteristics of PASC. (Gagiannis *et al.*, 2023)

This cohort comprises 51 patients, averaging 40 years of age, with 43% female. They showcased symptoms an average of 17 weeks post a mild COVID-19 infection, with none requiring hospitalization. This study was conducted before the availability of vaccinations. High-resolution computed Tomography scans (HR-CT), transbronchial biopsies, and comprehensive clinical examinations were performed. Reverse Transcription Polymerase Chain Reaction (RT-PCR) and immunohistochemistry (nucleocapsid/spike/CD3/CD4/CD8) were also executed to detect persistent viral material and T-lymphocyte subtypes. Immunofluorescence multiplex and transmission electron microscopy (TEM) were completed to identify fibrin deposition and related macrophage subtypes. Cytokines in the broncho-alveolar lavage (BAL) fluid were examined using Legendplex immunoassays. (Gagiannis *et al.*, 2023)

The predominant symptoms within this cohort, dyspnea on exertion, could not be associated with significant spiroergometric or radiologic outcomes. A Forced Expiratory Volume in one second (FEV1) below 80% was seen in 15.7% of patients and a Low Attenuation Volume (LAV) above 5% in 35.5% of this cohort. The oxygen pulse showed improvement over time post-COVID-19 infection, reaching statistical significance ($p=0.0009$). Residual viral fragments were identified in only one patient. Although this parameter did not reach statistical significance, it's noteworthy that the T-cell concentration within the small airways diminished in the weeks following infection. Histopathological findings characterized PASC with fibrinous alveolitis, organizing pneumonia (OP), and T-cell infiltrates in the small airways. Interstitial

fibrin deposition wand pro-fibrotic macrophages (CD68/CD163/S100A9) were identified The H-scores of said macrophages could not be correlated to the severity of disease progression. (Gagiannis *et al.*, 2023)

The clinical manifestations of PASC varied, yet many patients experienced diminished lung functionality, characterized by decreased FEV1, Forced Vital Capacity (FVC), and airway obstruction resulting in an increased LAV. High levels of IL-1β cytokines and CD4+ lymphocytes in the bronchioles indicate inflammatory processes. Furthermore, subjects exhibited fibrotic tissue remodeling and organizing pneumonia. Despite similarities in symptomatic patterns and HR-CT attributes, the serological criteria for a connective tissue disease-associated interstitial lung disease/IPAF (CTD-ILD/IPAF) diagnosis were unmet. Except for one outlier, the viral matter could not be associated with pathological processes, challenging the hypothesis that unresolved viral presence is the cause of chronic inflammation. The observations suggest that PASC represents a post-viral pathological process driven by bronchiolitis. The histological, serological, and radiological results within this PASC cohort align with the criteria of bronchiolitis following a mild COVID-19 infection. Given the proven fibrotic deposition via transmission electron microscopy, profibrotic macrophages, and IL-1β cytokines in BAL fluid, it is concluded that continuous monitoring of PASC patients is imperative to observe the progression of pulmonary fibrosis. (Gagiannis *et al.*, 2023)

6.0.0 Bibliography

1. Aiyegbusi OL, Hughes SE, Turner G, Rivera SC, McMullan C, Chandan JS, Haroon S, Price G, Davies EH, Nirantharakumar K, Sapey E, Calvert MJ (2021) Symptoms, complications and management of long COVID: a review. J R Soc Med 114: 428–442. doi: 10.1177/01410768211032850

2. Borthwick LA, Wynn TA, Fisher AJ (2013) Cytokine-mediated tissue fibrosis. Biochim Biophys Acta 1832: 1049–1060. doi: 10.1016/j.bbadis.2012.09.014

3. Cevik M, Kuppalli K, Kindrachuk J, Peiris M (2020) Virology, transmission, and pathogenesis of SARS-CoV-2. BMJ 371: m3862. doi: 10.1136/bmj.m3862

4. Cheon IS, Li C, Son YM, Goplen NP, Wu Y, Cassmann T, Wang Z, Wei X, Tang J, Li Y, Marlow H, Hughes S, Hammel L, Cox TM, Goddery E, Ayasoufi K, Weiskopf D, Boonyaratanakornkit J, Dong H, Li H, Chakraborty R, Johnson AJ, Edell E, Taylor JJ, Kaplan MH, Sette A, Bartholmai BJ, Kern R, Vassallo R, Sun J (2021) Immune signatures underlying post-acute COVID-19 lung sequelae. Science Immunology 6: eabk1741. doi: 10.1126/sciimmunol.abk1741

5. Crook H, Raza S, Nowell J, Young M, Edison P (2021) Long covid-mechanisms, risk factors, and management. BMJ 374: n1648. doi: 10.1136/bmj.n1944.

6. Cui J, Li F, Shi Z-L (2019) Origin and evolution of pathogenic coronaviruses. Nat Rev Microbiol 17: 181–192. doi: 10.1038/s41579-018-0118-9

7. Dueck NP, Epstein S, Franquet T, Moore CC, Bueno J (2021) Atypical Pneumonia: Definition, Causes, and Imaging Features. Radiographics 41: 720–741. doi: 10.1148/rg.2021200131

8. El-Sayed A, Kamel M (2021) Coronaviruses in humans and animals. the role of bats in viral evolution. Environ Sci Pollut Res 28: 19589–19600. doi: 10.1007/s11356-021-12553-1

9. Ständiger Arbeitskreis der Kompetenz- und Behandlungszentren für Krankheiten durch hochpathogene Erreger am Robert Koch-Institut (STAKOB): Hinweise zu Erkennung, Diagnostik und Therapie von Patienten mit COVID-19. https://www.rki.de/DE/Content/Kommissionen/Stakob/Stellungnahmen/Stellungnahme-Covid-19_Therapie_Diagnose.pdf?__blob=publicationFile (08.03.2023)

10. ECDC European Centre for Disease Prevention and Control: Factsheet on COVID-19. https://www.ecdc.europa.eu/en/infectious-disease-topics/z-disease-list/covid-19/factsheet-covid-19. (03.11.2023)

11. Frickmann H, Jungblut S, Hirche TO, Groß U, Kuhns M, Zautner AE (2012) The influence of virus infections on the course of COPD. Eur J of Microbiol Immunol 2: 176–185. doi: 10.1556/EuJMI.2.2012.3.2

12. Gagiannis D, Czech A, Steinestel K (2022) Post-COVID: The multimodal path to the right treatment strategy. ERJ Open Research 8: 80. doi: 10.1183/23120541.LSC-2022.80

13. Gagiannis D, Hackenbroch C, Bloch W, Zech F, Kirchhoff F, Djudjaj S, Stillfried S, Bülow R, Boor P, Steinestel K (2023) Clinical, imaging, serological, and histopathological features of pulmonary post-acute sequelae after mild COVID-19 (PASC). Am J of Respir Crit Care Med 5: 618-621. doi: 10.1164/rccm.202302-0285LE

14. Gagiannis D, Hackenbroch C, Czech A, Lindner A, Maag N, Bloch W, Zech F, Kirchhoff F, Djudjaj S, Stillfried S von, Bülow R, Boor P, Steinestel K: Clinical, imaging, serological, and histopathological features of pulmonary post-acute sequelae after mild COVID-19 (PASC). MedRxiv (Preprint). https://www.medrxiv.org/content/10.1101/2022.11.29.22282913v1 (08.03.2023)

15. Gagiannis D, Umathum VG, Bloch W, Rother C, Stahl M, Witte HM, Djudjaj S, Boor P, Steinestel K (2021) Antemortem vs Postmortem Histopathologic and Ultrastructural Findings in Paired Transbronchial Biopsy Specimens and Lung Autopsy Samples From Three Patients With Confirmed SARS-CoV-2. Am J Clin Pathol 157: 54–63. doi: 10.1093/ajcp/aqab087.

16. Hammad H, Lambrecht BN (2021) The basic immunology of asthma. Cell 184: 1469–1485. doi: 10.1016/j.cell.2021.04.019

17. Hansbro NG, Horvat JC, Wark PA, Hansbro PM (2008) Understanding the mechanisms of viral induced asthma: new therapeutic directions. Pharmacol Ther 117: 313–353. doi: 10.1016/j.pharmthera.2007.11.002

18. Harrison NL, Sachs JD (2022) A call for an independent inquiry into the origin of the SARS-CoV-2 virus. Proc Natl Acad Sci U S A 119: e2202769119. doi: 10.1073/pnas.2202769119

19. Jacobs JJL (2021) Persistent SARS-2 infections contribute to long COVID-19. Med Hypotheses 149: 110538. doi: 10.1016/j.mehy.2021.110538

20. Kamp JC, Werlein C, Plucinski EKJ, Neubert L, Welte T, Lee PD, Tafforeau P, Walsh C, Kuehnel MP, Schuppan D, Hoeper MM, Jonigk DD, Ackermann M (2023) Novel Insight into Pulmonary Fibrosis and Long COVID. m J Respir Crit Care Med 207: 1105–1107. doi: 10.1164/rccm.202212-2314LE

21. Kim EA, Lee KS, Primack SL, Yoon HK, Byun HS, Kim TS, Suh GY, Kwon OJ, Han J (2002) Viral Pneumonias in Adults: Radiologic and Pathologic Findings. RadioGraphics 22: 137–149. doi: 10.1148/radiographics.22.suppl_1.g02oc15s137

22. Kinkade S, Long NA (2016) Acute Bronchitis. Am Fam Physician 94: 560–565.

23. Littlefield KM, Watson RO, Schneider JM, Neff CP, Yamada E, Zhang M, Campbell TB, Falta MT, Jolley SE, Fontenot AP, Palmer BE (2022) SARS-CoV-2-specific T cells associate with inflammation and reduced lung function in pulmonary post-acute sequalae of SARS-CoV-2. PLoS Pathog 18: e1010359. doi: 10.1371/journal.ppat.1010359

24. Lungeninformationsdienst: Lungenentzündung: Symptome und Grundlagen. https://www.lungeninformationsdienst.de/krankheiten/lungenentzuendung/grundlagen. (03.11.2023)

25. Luyt C-É, Combes A, Trouillet J-L, Nieszkowska A, Chastre J (2011) Virus-induced acute respiratory distress syndrome: epidemiology, management and outcome. Presse Med 40: e561-e568. doi: 10.1016/j.lpm.2011.05.027

26. Martina L-S (2020) Long COVID: Der lange Schatten von COVID-19. Dtsch Arztebl Int117: A2416-A2420.

27. Masters PS (2006) The molecular biology of coronaviruses. Adv Virus Res 66: 193–292.

28. Menni C, Valdes AM, Polidori L, Antonelli M, Penamakuri S, Nogal A, Louca P, May A, Figueiredo JC, Hu C, Molteni E, Canas L, Österdahl MF, Modat M, Sudre CH, Fox B, Hammers A, Wolf J, Capdevila J, Chan AT, David SP, Steves CJ, Ourselin S, Spector TD (2022) Symptom prevalence, duration, and risk of hospital admission in individuals infected with SARS-CoV-2 during periods of omicron and delta variant dominance: a prospective observational study from the ZOE COVID Study. Lancet 399: 1618–1624. doi: 10.1016/S0140-6736(22)00327-0

29. Menni C, Valdes AM, Polidori L, Antonelli M, Penamakuri S, Nogal A, Louca P, May A, Figueiredo JC, Hu C, Molteni E, Canas L, Österdahl MF, Modat M, Sudre CH, Fox B, Hammers A, Wolf J, Capdevila J, Chan AT, David SP, Steves CJ, Ourselin S, Spector TD (2022) Symptom prevalence, duration, and risk of hospital admission in individuals infected with SARS-CoV-2 during periods of omicron and delta variant dominance: a prospective observational study from the ZOE COVID Study - Appendix p5. Lancet 399: 8–11. doi: 10.1016/S0140-6736(22)00327-0

30. Merad M, Blish CA, Sallusto F, Iwasaki A (2022) The immunology and immunopathology of COVID-19. Science 375: 1122–1127. doi: 10.1126/science.abm8108.

31. Mittal A, Manjunath K, Ranjan RK, Kaushik S, Kumar S, Verma V (2020) COVID-19 pandemic: Insights into structure, function, and hACE2 receptor recognition by SARS-CoV-2. PLoS Pathog 16: e1008762. doi: 10.1371/journal.ppat.1008762.

32. Myall KJ, Mukherjee B, Castanheira AM, Lam JL, Benedetti G, Mak SM, Preston R, Thillai M, Dewar A, Molyneaux PL, West AG (2021) Persistent Post-COVID-19 Interstitial Lung Disease. An Observational Study of Corticosteroid Treatment. Ann Am Thorac Soc18: 799–806. doi: 10.1513/AnnalsATS.202008-1002OC

33. National Heart, Lung, and Blood Institute: Acute Respiratory Distress Syndrome (ARDS) https://www.nhlbi.nih.gov/health/ards (07.11.2023)
- Symptoms: Signs and symptoms of ARDS https://www.nhlbi.nih.gov/health/ards/symptoms (07.11.2023)

- Diagnosis: How ARDS is diagnosed https://www.nhlbi.nih.gov/health/ards/diagnosis (07.11.2023)

- Causes and Risk Factors: Causes and risk factors of ARDS https://www.nhlbi.nih.gov/health/ards/causes-and-risk-factors (07.11.2023)

- Treatment: How ARDS is treated https://www.nhlbi.nih.gov/health/ards/treatment (07.11.2023)

- Living with: Living with ARDS https://www.nhlbi.nih.gov/health/ards/living-with (07.11.2023)

34. National Institute for Health and Care Excellence (NICE): COVID-19 rapid evidence review: Signs, symptoms and prevalence. https://files.magicapp.org/guideline/08d10c67-1331-4146-9471-b15d1d93e707/files/Evidence_review__signs_symptoms_prevalence_FINAL_r400908.pdf (03.07.2023)

35. National Institute for Health and Care Excellence (NICE): COVID-19 rapid guideline: managing the long-term effects of COVID-19. https://www.ncbi.nlm.nih.gov/books/NBK567261/ (01.05.2023)

36. National Institute for Health and Care Excellence (NICE): Asthma: diagnosis, monitoring and chronic asthma management. https://www.nice.org.uk/guidance/ng80/resources/asthma-diagnosis-monitoring-and-chronic-asthma-management-pdf-1837687975621 (07.05.2023)

37. Obar JJ, Shepardson KM: Coinfections in the lung: How viral infection creates a favorable environment for bacterial and fungal infections (2023) PLoS Pathog 19: e1011334. doi: 10.1371/journal.ppat.1011334

38. Padem N, Saltoun C (2019) Classification of asthma. Allergy Asthma Proc 40: 385–388. doi: 10.2500/aap.2019.40.4253

39. Papazian L, Calfee CS, Chiumello D, Luyt C-E, Meyer NJ, Sekiguchi H, Matthay MA, Meduri GU (2016) Diagnostic workup for ARDS patients. Intensive Care Med 42: 674–685. doi: 10.1007/s00134-016-4324-5

40. Płóciniczak A, Goździk-Spychalska J, Batura-Gabryel HB-G (2017) Interstitial pneumonia with autoimmune features (IPAF) and radiological findings suggestive of lymphocytic interstitial pneumonia (LIP) - case report. Adv Respir Med 85: 46–50. doi: 10.5603/ARM.2017.0009

41. Proal AD, VanElzakker MB (2021) Long COVID or Post-acute Sequelae of COVID-19 (PASC): An Overview of Biological Factors That May Contribute to Persistent Symptoms. Front Microbiol 12: 698169. doi: 10.3389/fmicb.2021.698169

42. RECOVERY Collaborative Group, Horby P, Lim WS, Emberson JR, Mafham M, Bell JL, Linsell L, Staplin N, Brightling C, Ustianowski A, Elmahi E, Prudon B, Green C, Felton T, Chadwick D, Rege K, Fegan C, Chappell LC, Faust SN, Jaki T, Jeffery K, Montgomery A, Rowan K, Juszczak E, Baillie JK, Haynes R, Landray MJ (2021) Dexamethasone in Hospitalized Patients with Covid-19. N Engl J Med 384: 693–704. doi: 10.1056/NEJMoa2021436

43. Riefaie E (2020) Covid-19 treatment approaches. Masterthesis, Universität Wien

44. Ryu JH, Azadeh N, Samhouri B, Yi E (2020) Recent advances in the understanding of bronchiolitis in adults. F1000Res 9: 568. doi: 10.12688/f1000research.21778.1

45. Ryu JH, Myers JL, Swensen SJ (2003) Bronchiolar disorders. Am J Respir Crit Care Med 168: 1277–1292. doi: 10.1164/rccm.200301-053SO

46. Shang J, Wan Y, Luo C, Ye G, Geng Q, Auerbach A, Li F (2020) Cell entry mechanisms of SARS-CoV-2. Proc Natl Acad Sci U S A 117: 11727–11734. doi: 10.1073/pnas.2003138117

47. Shanmugam C, Mohammed AR, Ravuri S, Luthra V, Rajagopal N, Karre S (2020) COVID-2019 - A comprehensive pathology insight. Pathol Res Pract 216: 153222. doi: 10.1016/j.prp.2020.153222

48. Sohrabi C, Alsafi Z, O'Neill N, Khan M, Kerwan A, Al-Jabir A, Iosifidis C, Agha R (2020) World Health Organization declares global emergency: A review of the 2019 novel coronavirus (COVID-19). Int J Surg 76: 71–76. doi: 10.1016/j.ijsu.2020.02.034

49. Son K, Jamil R, Chowdhury A, Mukherjee M, Venegas C, Miyasaki K, Zhang K, Patel Z, Salter B, Yuen ACY, Lau KS-K, Cowbrough B, Radford K, Huang C, Kjarsgaard M, Dvorkin-Gheva A, Smith J, Li Q-Z, Waserman S, Ryerson CJ, Nair P, Ho T, Balakrishnan N, Nazy I, Bowdish DME, Svenningsen S, Carlsten C, Mukherjee M (2023) Circulating anti-nuclear autoantibodies in COVID-19 survivors predict long COVID symptoms. Eur Respir J 61: 2200970. doi: 10.1183/13993003.00970-2022

50. Steinestel K, Czech A, Hackenbroch C, Bloch W, Gagiannis D (2021) Klinische, radiologische und histopathologische Merkmale des pulmonalen Post-COVID-Syndroms. Pathologe 42:160–164. doi: 10.1007/s00292-021-01024-6

51. Su S, Wong G, Shi W, Liu J, Lai ACK, Zhou J, Liu W, Bi Y, Gao GF (2016) Epidemiology, Genetic Recombination, and Pathogenesis of Coronaviruses. Trends Microbiol 24: 490–502. doi: 10.1016/j.tim.2016.03.003

52. Torres-Castro R, Vasconcello-Castillo L, Alsina-Restoy X, Solis-Navarro L, Burgos F, Puppo H, Vilaró J (2021) Respiratory function in patients post-infection by COVID-19: A systematic review and meta-analysis. Pulmonology 27: 328–337. doi: 10.1016/j.pulmoe.2020.10.013

53. Trinkmann F, Müller M, Reif A, Kahn N, Kreuter M, Trudzinski F, Eichinger M, Heussel C-P, Herth FJF (2021) Residual symptoms and lower lung function in patients recovering from SARS-CoV-2 infection. Eur Respir J 57: 2003002. doi: 10.1183/13993003.03002-2020

54. WHO Rapid Evidence Appraisal for COVID-19 Therapies (REACT) Working Group, Sterne JAC, Murthy S, Diaz JV, Slutsky AS, Villar J, Angus DC, Annane D, Azevedo LCP, Berwanger O, Cavalcanti AB, Dequin P-F, Du B, Emberson J, Fisher D, Giraudeau B, Gordon AC, Granholm A, Green C, Haynes R, Heming N, Higgins JPT, Horby P, Jüni P, Landray MJ, Le Gouge A, Leclerc M, Lim WS, Machado FR, McArthur C, Meziani F, Møller MH, Perner A, Petersen MW, Savovic J, Tomazini B, Veiga VC, Webb S, Marshall JC (2020) Association Between Administration of Systemic Corticosteroids and Mortality Among Critically Ill Patients With COVID-19: A Meta-analysis. JAMA 324: 1330–1341. doi: 10.1001/jama.2020.17023

55. Widders A, Broom A, Broom J (2020) SARS-CoV-2: The viral shedding vs infectivity dilemma. Infect Dis Health 25: 210–215. doi: 10.1016/j.idh.2020.05.002

56. Worobey M, Levy JI, Malpica Serrano L, Crits-Christoph A, Pekar JE, Goldstein SA, Rasmussen AL, Kraemer MUG, Newman C, Koopmans MPG, Suchard MA, Wertheim JO, Lemey P, Robertson DL, Garry RF, Holmes EC, Rambaut A, Andersen KG (2022) The Huanan Seafood Wholesale Market in Wuhan was the early epicenter of the COVID-19 pandemic. Science 377: 951–959. doi: 10.1126/science.abp8715

57. Xu Z, Shi L, Wang Y, Zhang J, Huang L, Zhang C, Liu S, Zhao P, Liu H, Zhu L, Tai Y, Bai C, Gao T, Song J, Xia P, Dong J, Zhao J, Wang F-S (2020) Pathological findings of COVID-19 associated with acute respiratory distress syndrome. Lancet Respir Med 8: 420–422. doi: 10.1016/S2213-2600(20)30076-X

58. Yong SJ: Long COVID or post-COVID-19 syndrome (2021) putative pathophysiology, risk factors, and treatments. Infect Dis (Lond) 53: 737–754. doi: 10.1080/23744235.2021.1924397

Appendix

List of Tables

Table 1 Classification of the progression severity of acute COVID-19 with definitions defined by the RKI and description of symptoms. ((STAKOB), 2023) _____ 10

Table 2 Clinical case definitions to diagnose acute COVID-19 (Coronavirus Disease 2019), ongoing symptomatic of COVID-19, and post-COVID-19, as well as the definition of long-covid as per the guidelines (National Institute for Health and Care Excellence (NICE) et al., 2022) _____ 12

Table 3 Organ-specific symptoms through their Angiotensin-Converting Enzyme 2 - Receptor pathway after COVID-19 (Coronavirus Disease 2019) infection. (Crook et al., 2021). _____ 14

Table 4 Classification of bronchial abnormalities as proposed by Ryu (Ryu, Myers and Swensen, 2003)_____ 20

Table 5 Criteria for the new proposition of the term Interstitial Pneumonia with Autoimmune Features (IPAF) in the clinical, serologic and morphologic domain (Płóciniczak, Goździk-Spychalska and Batura-Gabryel, 2017)._____ 22

Table 6 Measured parameters during Spiroergometry. _____ 29

Table 7 Baseline clinical characteristics and assessment of lung function in PASC Patients, University Hospital Ulm, 2020-2022. PASC. We can see an increase in the FVC, FEV1, and a decrease in the VO2/HF. Forced vital capacity (FVC), total lung capacity (TLC), forced expiratory volume in one second (FEV1), diffusing capacity of the lung for carbon monoxide (DLCO), bronchoalveolar lavage (BAL), interquartile range (IQR), maximal expiratory flow at 50% of forced vital capacity (MEF50), lung attenuation value (LAV), post-acute sequelae of COVID-19 (PASC) _____ 37

Table 8 Lung histology and spatial T lymphocyte subtyping in 51 post-COVID patients and pre-pandemic autopsy controls, University Hospital Ulm, 2020-2021. Post-acute Sequelae of SARS-CoV-2 (PASC), Cluster of Differentiation 4 positive (CD4+), Cluster of Differentiation 8 positive (CD8+), Interquartile Range (IQR), Transmission electron microscopy (TEM) _____ 40

Table 9 Macrophage panel staining and automated quantitative imaging. H-scores (CD16/CD68/CD163/S100A9) and CD cell concentrations in 38 PASC patients, University Hospital Ulm, 2020-2021. Post-acute sequelae of COVID-19 (PASC), Cluster of Differentiation (CD)_____ 46

List of Figures

Figure 1 The viral taxonomy of SARS-CoV-2 subcategorized into family, subfamily, genus, and species. _____ *2*

Figure 2 The structure of a spike protein (S). _____ *3*

Figure 3 Structure of the Severe Acute Respiratory Syndrome Coronavirus 2 (Sars-CoV-2) Virion _____ *4*

Figure 4 Comparison of the symptomatic distribution in pre-Omicron (blue) and Omicron (grey) cases categorized into predominant symptoms, the data set is based on a cohort that received 2 vaccinations during the evaluation. _____ *8*

Figure 5 Prevalence of common symptoms of COVID-19 *(Coronavirus Disease 2019) within three different time frames (0-4 weeks, 4-12 weeks and 12+ weeks) (National Institute for Health and Care Excellence, 2021)* _____ *13*

Figure 6 Workflow of the diagnostic scheme used to select the PASC patient cohort, University Hospital Ulm, 2020-2022. *66 PASC-ILD patients were admitted to the study. These underwent physical examinations, spiroergometry and a medical history evaluation. 51 out of these 61 patients were then admitted to HRCT/BAL/Biopsies. 11 were subsequently moved on to Transmission Electron Microscopy (TEM), 35 into immunohistochemistry (IHC), 36 into Reverse Transcription Polymerase Chain Reaction (RT-PCR), 38 into multi-immunohistochemistry (IHC), and one into fluorescence in situ hybridization (FISH).* _____ *35*

Figure 7 Clinical, histopathological, serological, and radiological results of 51 PASC subjects between 2 and 55 weeks since COVID, University Hospital Ulm, 2020-22*.* _____ *36*

Figure 8 *Improvement of VO2/HF and RV over weeks in patients since COVID-19 infection (0-60 weeks), University Hospital Ulm, 2020-2022. Coronavirus Disease 2019 (COVID-19), Residual volume (RV), oxygen consumption over heart rate (VO2/HF), weeks (wks)* _____ *38*

Figure 9 Radiological results showing the ground-glass opacities (arrowheads) and reticulations in PASC patients (right), in contrast to Acute COVID-19 patients (left), University Hospital Ulm, 2020-2022. *Post-acute Sequelae of SARS-CoV-2 (PASC), Coronavirus Disease 2019 (COVID-19)* _____ *39*

Figure 10 Lung tissue biopsies of PASC patients in H.E. and Masson-Goldner staining, University Hospital Ulm, 2020-2021. *In the H.E. stained biopsy tissues shown on the left, arrows indicate organizing pneumonia (triangle tip) and alveolar fibrinous exudate (straight arrows). The image on the right illustrates interstitial lymphocytosis. The Masson-Goldner stained image clearly demonstrates minimal interstitial fibrosis. The scale bar represents 100µm. Post-acute Sequelae of SARS-CoV-2 (PASC), Hematoxylin and Eosin staining (H.E.)* _____ *41*

Figure 11 Immunohistochemistry of lung tissue in PASC and COVID-19 biopsies, University Hospital Ulm, 2020-2021. *N,S proteins and the RT-PCR for the RdRp gene were negative in the immunohistochemistry. One subject tested positive in the RT-PCR for the E-gene which was later confirmed in the FISH-analysis. Post-acute Sequelae of SARS-CoV-2 (PASC), immunohistochemistry (IHC), Fluorescence In Situ Hybridization (FISH), Coronavirus Disease 2019 (COVID-19), Severe Acute Respiratory Syndrome Coronavirus 2(SARS-CoV-2).* _____ *42*

Figure 12 Comparison of the T cell, CD4+ T-cell, CD8+ T-cell and CD4/CD8 ratio in PASC patients and autopsy controls in the small airways in interstitium, University Hospital Ulm, 2020-2021*. All parameters are elevated in PASC patients, in both the small airways and interstitium. The concentration of CD3+ and CD4+ T-helper cells in the small airways is notably higher compared, to the interstitium in PASC patients and both airways and the interstitium in autopsy controls. Cluster of Differentiation 4 positive (CD4+), Cluster of Differentiation 8 positive (CD8+), Post-acute Sequelae of SARS-CoV-2 (PASC), Air condition (AC), Bronchoalveolar lavage (BAL)* _____ *43*

Figure 13 Spatial distribution of CD4+ and CD8+ T cells within the lower and middle lobe of the lung, University Hospital Ulm, 2020-2021. *Middle lobe (ML), Lower lobe (LL), Cluster of Differentiation 4,8 positive (CD4/8+), Post-acute Sequelae of SARS-CoV-2 (PASC)* _____ *44*

Figure 14 Microphotographs of immunochemically double-stained cells in PASC biopsies of the small airways and interstitium, University Hospital Ulm, 2020-2021*. On the left are CD3-cells, followed by CD4/CD8 around the bronchioli, and CD4/CD8 in the interstitium on the right. The scale bar represents 100µm. Cluster of Differentiation 3,4,8 positive (CD3/4/8+), Post-acute Sequelae of SARS-CoV-2 (PASC),* _____ *44*

Figure 15 Microphotograph transmission electron microscopy of lung tissue in PASC patients to demonstrate collagen fibrils (*) in 11 of 14 patients, University Hospital Ulm,2021-2022. *Alveolus (A)*_____ *45*

Figure 16 H-Scores for the pro-fibrotic macrophages (CD68/CD163/S100A9) and CD4+/CD8+ around the airways and alveolar septa in PASC biopsies, University Hospital Ulm, 2020-2021. *Cluster of Differentiation 4/8 positive (CD4+/CD8+),* __ *46*

Figure 17 Levels of H-scores of pro-fibrotic macrophages CD68/CD163/S100A9 and CD4+/CD8+ in the small airways and interstitium of PASC patients, University Hospital Ulm, 2020-2021. *Middle lobe (ML), Lower lobe (LL), bronchoalveolar lavage (BAL), Diffusing Capacity of the Lung for Carbon Monoxide (DLCO), oxygen consumption over heart rate (VO2/HF)* _____ *47*

Figure 18 Interleukin levels in BAL Fluid of PASC and control patients were tested using legendary immunoplex essays, University Hospital Ulm, 2020-2021*. The levels of IL-8, TNF-α, IL-6, IL-1β, and IFN-Λ1 were determined. IL1-β and IL-8 were increased in comparison to controls. However, the parameter could not reach statistical significance. Interleukin (IL), Tumor necrosis factor-alpha (TNF-α), interferon delta 1 (IFN-Y1), post-acute sequelae of COVID-19 (PASC), control (ctrl.)* _____ *48*

Acknowledgment

I sincerely thank my supervisor, Prof. Dr. med. Dr. rer. nat. Konrad Steinestel, for his steadfast support and invaluable guidance during my thesis journey.
I am also grateful to the team for their hard work and perseverance, especially during the pandemic's challenges.
A special note of thanks goes to Dr. med. Daniel Gagiannis for his dedicated data collection and organization assistance.
Thank you to my family.

Curriculum Vitae

For reasons of protection of personal data this page was removed.

Publications/Preprints/Posters

Gagiannis D, Czech A, Steinestel K (2022) Post-COVID: The multimodal path to the right treatment strategy. ERJ Open Research 8: 80. doi: 10.1183/23120541.LSC-2022.80

Gagiannis D, Hackenbroch C, Czech A, Lindner A, Maag N, Bloch W, Zech F, Kirchhoff F, Djudjaj S, Stillfried S von, Bülow R, Boor P, Steinestel K: Clinical, imaging, serological, and histopathological features of pulmonary post-acute sequelae after mild COVID-19 (PASC). MedRxiv (Preprint). https://www.medrxiv.org/content/10.1101/2022.11.29.22282913v1 (08.03.2023)

Gagiannis D, Schmidt-Alba J, Czech A, Lindner A, Walter K, Stahl M, Steinestel K (2023) The Therapeutic Path in the Post-COVID Thicket - Renaissance of Azithromycin (abstract). American Journal of Respiratory and Critical Care Medicine 207: A6292

Gagiannis D, Steinestel K, Czech A, Hackenbroch C, Walter K, Lindner A (2022) Das “post COVID-Syndrom” – Psychosomatischer Diagnosetrend oder ein Fall für das ILD Board? Pneumologie 76: 15. doi: 10.1055/s-0042-1747720

Steinestel K, Czech A, Hackenbroch C, Bloch W, Gagiannis D (2021) Klinische, radiologische und histopathologische Merkmale des pulmonalen Post-COVID-Syndroms. Pathologe 42:160–164. doi: 10.1007/s00292-021-01024-6

Famulatur: Zu Corona-Zeiten in Südkorea. In: Das News-Portal der Zahnärztlichen Mitteilungen. https://www.zm-online.de/artikel/2020/licht-am-ende-des-tunnels/famulatur-zu-corona-zeiten-in-suedkorea. (06.11.2023)